Journal of Medicinal Chemistry

Article

pubs.acs.org/jmc

Design, Synthesis and Discovery of Picomolar Selective α4β2 Nicotinic Acetylcholine Receptor Ligands

Venkata M. Yenugonda,[†,∥] Yingxian Xiao,[‡] Edward D. Levin,[§] Amir H. Rezvani,[§] Thao Tran,[‡] Nour Al-Muhtasib,[‡] Niaz Sahibzada,[‡] Teresa Xie,[‡] Corinne Wells,[§] Susan Slade,[§] Joshua E. Johnson,[§] Sivanesan Dakshanamurthy,[†,∥] Hye-Sik Kong,[†,∥] York Tomita,[∥] Yong Liu,[†,∥] Mikell Paige,[†,∥] Kenneth J. Kellar,[‡] and Milton L. Brown*,[†,∥]

[†]Center for Drug Discovery, Georgetown University Medical Center, 3970 Reservoir Road NW, Research Building, EP-07, Washington, D.C. 20057, United States

[‡]Department of Pharmacology and Physiology, Georgetown University School of Medicine, Washington, D.C. 20057, United States

[§]Department of Psychiatry and Behavioral Sciences, Duke University Medical Center, Durham, North Carolina 27710, United States

[∥]Department of Oncology, Lombardi Comprehensive Cancer Center, Georgetown University Medical Center, 3970 Reservoir Road NW, Research Building, Washington, D.C. 20057, United States

Supporting Information

ABSTRACT: Developing novel and selective compounds that desensitize α4β2 nicotinic acetylcholine receptors (nAChRs) could provide new effective treatments for nicotine addiction, as well as other disorders. Here we report a new class of nAChR ligands that display high selectivity and picomolar binding affinity for α4β2 nicotinic receptors. The novel compounds have K_i values in the range of 0.031−0.26 nM and properties that should make them good candidates as drugs acting in the CNS. The selected lead compound **1** (VMY-2-95) binds with high affinity and potently desensitizes α4β2 nAChRs. At a dose of 3 mg/kg, compound **1** significantly reduced rat nicotine self-administration. The overall results support further characterizations of compound **1** and its analogues in preclinical models of nicotine addiction and perhaps other disorders involving nAChRs.

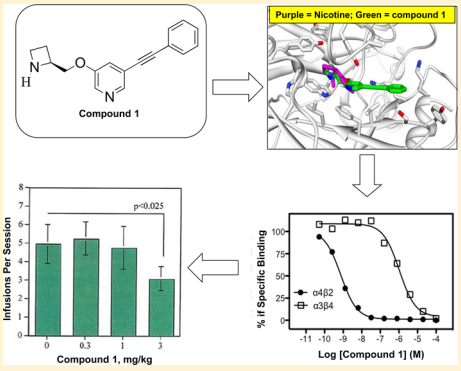

INTRODUCTION

Nicotinic acetylcholine receptors (nAChRs) are pentameric ligand gated ion channels with significant potential as molecular targets for drugs designed to treat a variety of central nervous system disorders.[1−4] In vertebrates, 12 neuronal nAChR subunits have been identified including nine alpha subunits (α2−α10) and three beta subunits (β2−β4).[5] These subunits may coassemble as either heteromeric and homomeric pentameric receptors, forming a theoretically large array of receptor subtypes.[6−8] The predominant nAChRs in the CNS are the heteromeric α4β2* subtype, composed of α4 and β2 subunits (the * indicates that some of these nAChRs may contain one or more other subunits) and the homomeric α7 subtype. Certain areas of brain also contain a high density of α3β4* nAChRs, and this subtype appears to be the predominant nAChR in several autonomic nervous system ganglia.[9]

Nicotine interacts with α4β2, α4β2α6*, and α7 nAChRs in the dopaminergic mesolimbic pathway, which connects the ventral tegmental area of the midbrain and the limbic system via the nucleus accumbens,[10] and these effects of nicotine on brain dopaminergic systems are important in reinforcing drug self-administration. The mesolimbic dopamine system is assumed to mediate the pleasurable and rewarding effects of most drugs of abuse, including nicotine.[11] There is convincing evidence from in vivo studies that mesolimbic α4β2* nAChRs play a pivotal role in nicotine self-administration in mice.[12−14] Furthermore, differential activation and desensitization of nAChR subtypes on dopamine and GABA neurons and possibly glutamate neurons results in stimulated dopamine release in the nucleus accumbens, leading to positive reinforcement of nicotine.[15]

The α4β2 subtype of nAChR serves as an important target for treating nicotine addiction as well as anxiety, depression, and cognitive disorders, and thus these receptors have been targeted with a wide array of compounds to develop potential therapies (Figure 1A). Many of the new compounds are structurally related to the natural nAChR ligands, including nicotine, epibatidine, and cytisine.

In 2006, varenicline (Figure 1A) emerged as the newest drug approved by U.S. FDA as a therapeutic aid for smoking cessation.[16] Clinical studies indicate that varenicline is the most effective drug currently available to help people stop

Received: June 6, 2013
Published: September 18, 2013

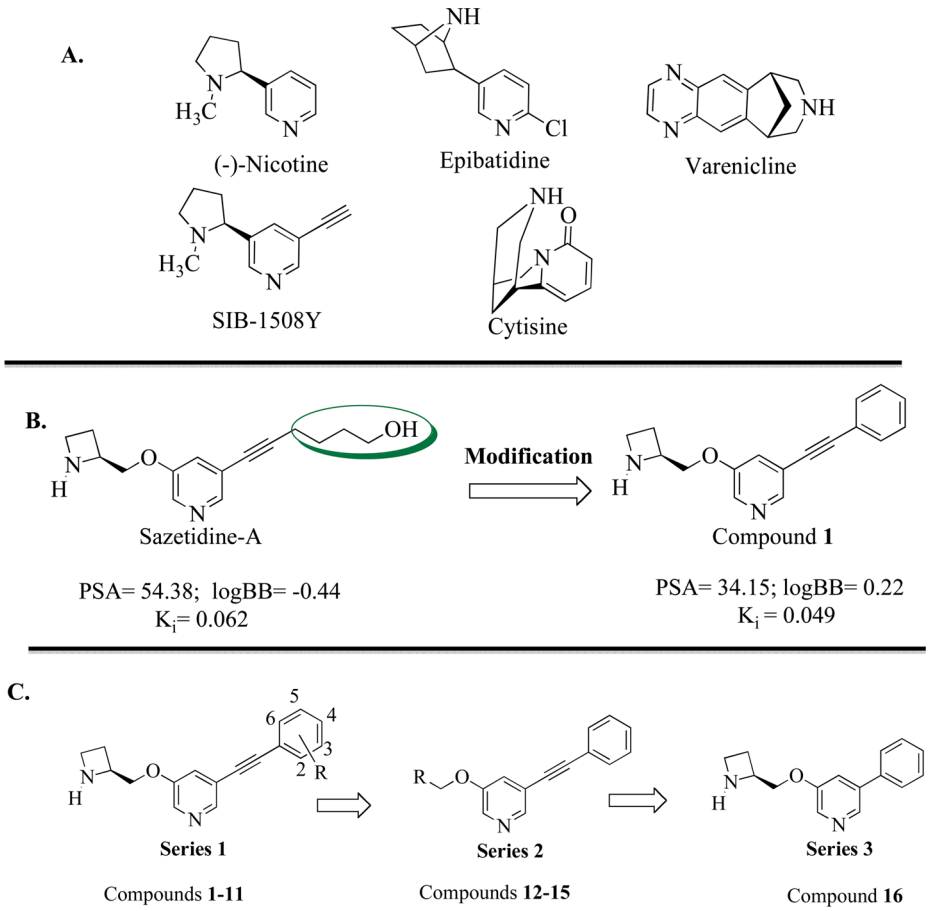

Figure 1. (A) Selected examples of natural and synthetic nAChR ligands. (B) Design strategy for compound **1**. (C) General structures of the present series of compounds.

smoking,[17−20] but its effects may be temporary.[17,18] Furthermore, varenicline shows notable adverse side effects that limit the use of this compound.[21] These side effects of varenicline are thought to be mediated predominantly through its action at non-$\alpha4\beta2$ receptors, most likely the $\alpha3\beta4$* and $\alpha7$ subtypes.[22,23] Pharmacological studies indicate that the interactions of varenicline with $\alpha4\beta2$ nAChRs play essential roles in the clinical effect of varenicline as a smoking cessation aid. In addition, varenicline also interacts with nAChRs containing $\alpha6$ and $\beta2$ subunits, which may also contribute to its effect.[24]

Xiao, et al. previously reported the synthesis and pharmacological properties of sazetidine (Saz-A) (Figure 1B), which potently and selectively desensitizes $\beta2$ containing nicotinic receptors, especially $\alpha4\beta2$ nAChRs, as measured by whole cell patch clamp and ion efflux assays.[25,26] In addition to its ability to cause long lasting desensitization of $\alpha4\beta2$ receptors, Saz-A also has agonist activity at the receptor subtype. It is highly interesting that Saz-A showed full agonist activity at the $(\alpha4)_2(\beta2)_3$ receptors but nearly no agonist activity at the $(\alpha4)_3(\beta2)_2$ receptors.[27] In the animal model, Saz-A reduced nicotine self-administration,[28] decreased alcohol intake,[29] and improved performance in tests of attention.[30] Saz-A was also found to produce behaviors consistent with potential antidepressant and/or antianxiety effects in rats and mice.[31−33] These promising in vivo results suggest that Saz-A is an excellent starting compound for developing additional potent and subtype-selective drugs that desensitize $\alpha4\beta2$ nAChRs. Recent in vivo studies showed a low concentration of Saz-A in rat brain,[33,34] suggesting that optimization of Saz-A physicochemical properties might enhance the in vivo CNS efficacy of this group of compounds.

In this report, we optimized the Saz-A ligand and provide the design, synthesis, and evaluation of a new class of picomolar active $\alpha4\beta2$ selective compounds. These compounds could lead to more effective treatments for nicotine addiction as well as other conditions that involve nAChRs.

■ RESULTS

Design and Synthesis of the New Nicotinic Ligands. Utilizing homologous series, we began our optimization of Saz-A by replacing the alkyl hydroxyl with a benzene group resulting in the design of compound **1** (Figure 1B). We anticipated that compound **1** would have an enhanced CNS profile based on the physicochemical properties of PSA (34.15), lipophilicity (log P = 2.36), and log BB (0.22). From our modeling studies (Figure 2), we envisioned that the benzene ring would provide more rigidity and favorable interactions with the $\alpha4\beta2$ nAChR subtype. Aromatic optimization of the benzene ring of compound **1** provided the compounds in series 1 (Figure 1C).

The compounds from route 1 were synthesized as shown in Scheme 1. Compound **18** was formed from a reaction of the 5-bromopyridin-3-ol **16** and the Boc-protected alcohol **17** under Mitsunobu conditions. Aromatic coupling of ethynyltrimethylsilane **19** to **18** resulted in the formation of **20**. Deprotection of TMS group in compound **20** resulted in the (*S*)-3-(azetidin-2-

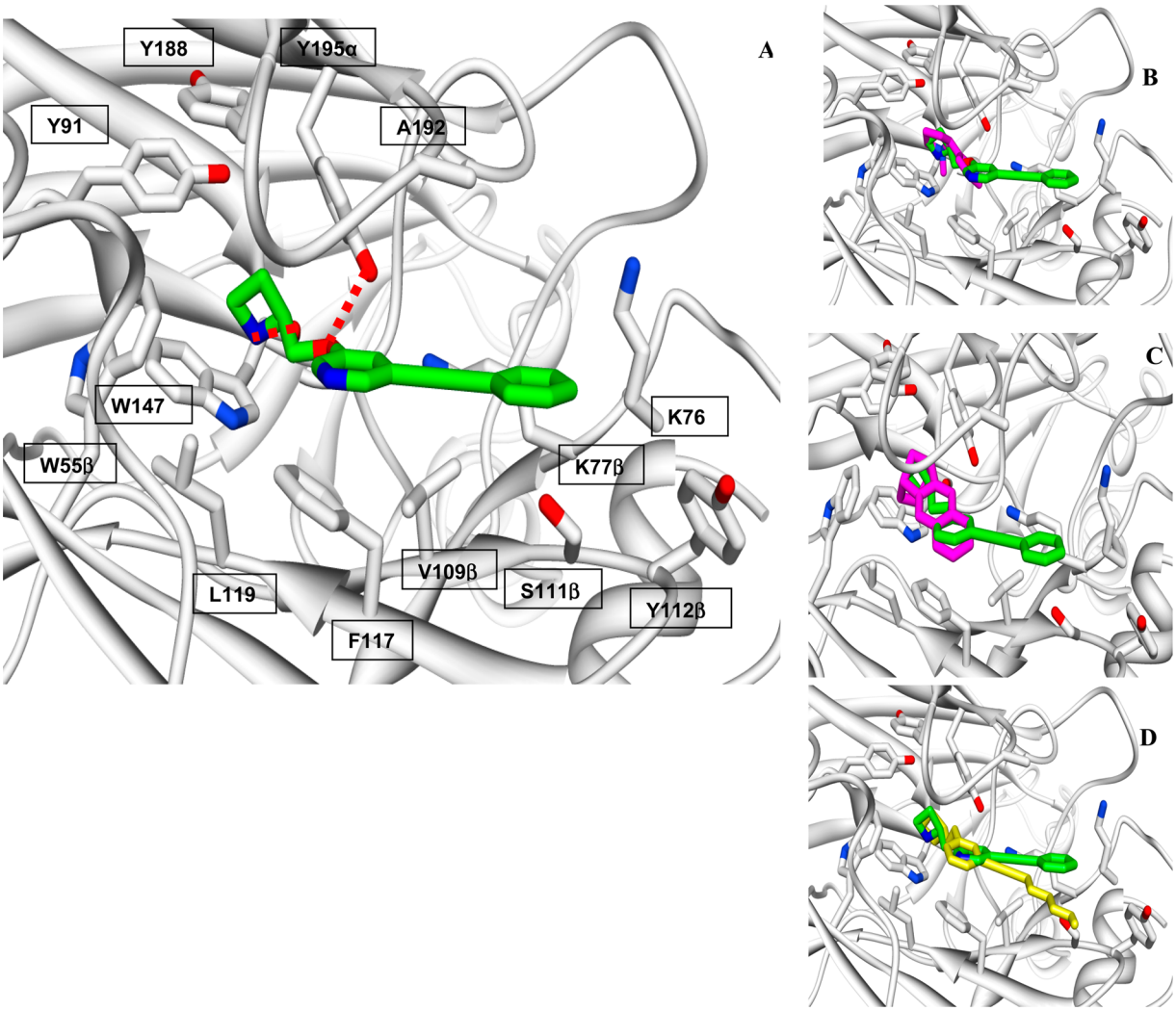

Figure 2. Predicted structural models of $\alpha4\beta2$ nAChR. (A) Atomic level interactions between compound **1** with $\alpha4\beta2$ nAChR. Binding site residues are labeled and shown in a stick model rendering. Molecular modeling overlay of compound **1** (colored green) with *S*-nicotine (B), varenecline (C), and Saz-A (D) in the $\alpha4\beta2$ nAChR binding site. Residues are labeled and shown in a stick model rendering.

ylmethoxy)-5-(phenylethynyl)pyridine **21**. Substituted aryl iodides were added to the intermediate **21** under Sonogashira reaction conditions to generate compounds **22**, **23**, **24**, and **25**. Subsequent deprotection of the Boc group yielded the final compounds (compound **1**, **2** (VMY-2-101), **3** (VMY-2-105), and **4** (VMY-2-109) in series 1.

With the success of the multistep route synthetic strategy, we optimized the chemical synthesis with a more efficient one-pot Sonogashira reaction[35] (Scheme 1, route 2) to generate the compounds in route 2. Synthesis of compounds **12** (VMY-2-161), **13** (VMY-2-177), and **14** (VMY-2-191) was accomplished by route 2 (Scheme 2A−C).

Compound **1** analogues were also designed and synthesized to investigate the importance of the azetidine ring, N-substitution, and stereochemistry on the binding affinity of ligands for nAChRs (Scheme 2). The *N*-methyl azetidine (**15**, VMY-2-205, Scheme 2D) was prepared by reductive methylation of the secondary amine with formaldehyde. Analogue compound **16** (VMY-2-203), a previously reported compound, was prepared as a standard to investigate the importance of a spacer group between the benzene and pyridine rings.[36] Compound **16** (Scheme 3) was synthesized by applying the Suzuki reaction to the Mitsunobu product (*S*)-*tert*-butyl 2-((5-bromopyridin-3-yloxy)methyl)azetidine-1-carboxylate (**18**) and phenylboronic acid (**41**), followed by Boc deprotection.

Binding Affinities for nAChR Subtypes. The binding affinities of all compounds synthesized for the receptor subtypes were examined in binding competition studies against [^{3}H]epibatidine. K_i values of these compounds at six defined subtypes of rat nAChRs are provided in Tables 1 and 2. Included in the tables are the K_i values in rat forebrain, which represents a mixture of more than one native nAChR.

All compounds in series 1 exhibited high affinity for the rat $\alpha4\beta2$ nAChR subtype with K_i values ranging from 0.031 nM compound **9** (VMY-2-131) to 0.26 nM compound **6** (VMY-2-117). These compounds also showed high affinities for the two other subtypes containing $\beta2$ subunits, $\alpha2\beta2$ and $\alpha3\beta2$ nAChRs. In contrast, the binding affinities of these compounds for nAChR subtypes containing $\beta4$ subunits are much lower than those for their $\beta2$ containing counterparts. As shown in Table 1, the selectivity of these compounds for $\alpha4\beta2$ receptors over $\alpha3\beta4$ receptors (K_i ratio) were very high, ranging from 5400 times compound **6** to 87000 times compound **7** (VMY-2-123). All of these ratios are much greater than that of nicotine or varenicline. Similar to the low affinities for $\alpha3\beta4$ receptors,

Scheme 1. Synthesis of Compounds in Series 1[a]

Route 1.

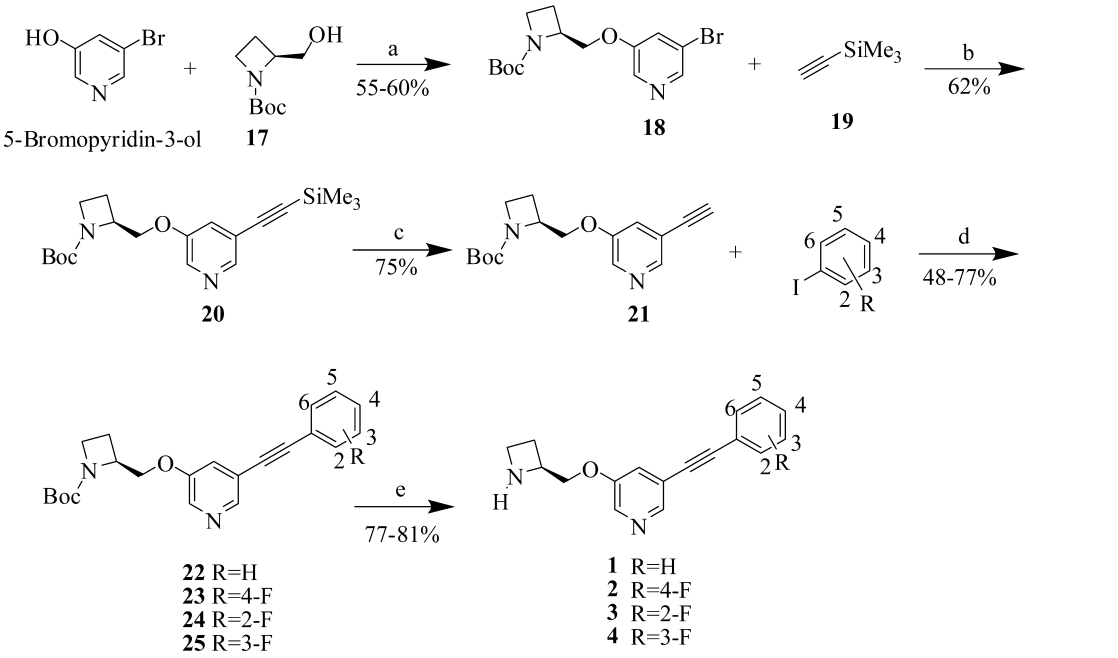

Route 2.

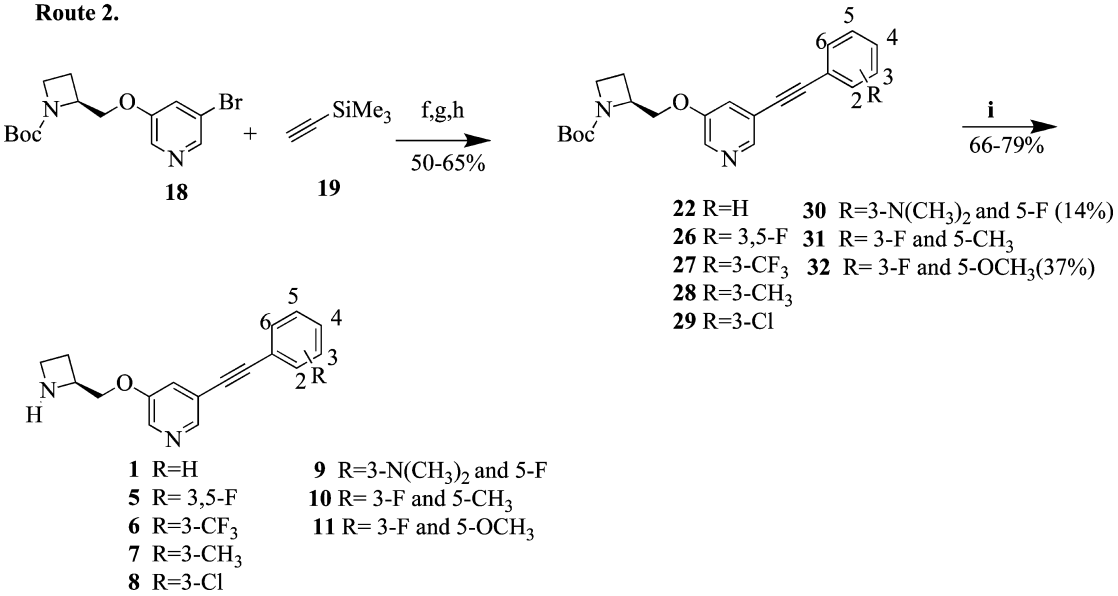

[a]Reagents and conditions: (a) DEAD, PPh_3, THF, O °C, 48 h; (b) 2 mol % $Pd(PPh_3)_2Cl_2$, 4 mol % PPh_3, 2 mol % CUI, iPr_2NH, toluene, 80 °C, 18 h; (c) KOH, MeOH/H_2O (20:1), 25 °C, 3 h; (d) 2 mol % $Pd(PPh_3)_2Cl_2$, 4 mol % PPh_3, 2 mol % CUI, iPr_2NH, toluene, 25 °C, 18 h; (e) TFA, CH_2Cl_2, 0 °C−rt 4−6 h then 2 M NaOH methanol in water (9:1), methanol, 18 h; (f) 4 mol% $Pd(PPh_3)_2Cl_2$, 8 mol % PPh_3, 8 mol% CUI, iPr_2NH, toluene, 80 °C, 18 h; (g) KOH, MeOH/H_2O (4:1), 25 °C, 3 h; (h) substituted aryl iodides, 25 °C, 16 h or substituted aryl bromide, 80 °C, 16 h; (i) TFA, CH_2Cl_2, 0 °C−rt , 4−6 h then 2M NaOH methanol in water (9:1), methanol, 18 h.

these compounds showed very low affinities for $\alpha7$ homomeric receptors (Table 1).

Because compound **1** showed a promising binding profile, we synthesized several analogues to evaluate the effects of substitutions on the benzene ring. Substitutions at position 2, 3, or 4 generated compounds **2**, **3**, **4**, **7**, and **8** (VMY-2-127). These singly substituted analogues have binding profiles similar to that of compound **1** (Table 1). The dual substituted analogues **5** (VMY-2-113), **9**, **10** (VMY-2-135), and **11**(VMY-2-139), also showed high affinities and selectivity for $\alpha4\beta2$ receptors. However, the installation of CF_3 at position 3 decreased the binding affinity for the $\alpha4\beta2$ receptor, as shown by the binding profile of **6**.

Interestingly, two compounds in series 2, compound **12** (azetidine replaced with cyclobutane) and compound **13** (ring opened analogue of azetidine), showed very low binding affinities to nAChRs (Table 2), indicating that the azetidine ring is important for the high affinity and selectivity binding

Scheme 2. Synthesis of Compounds in Series 2[a]

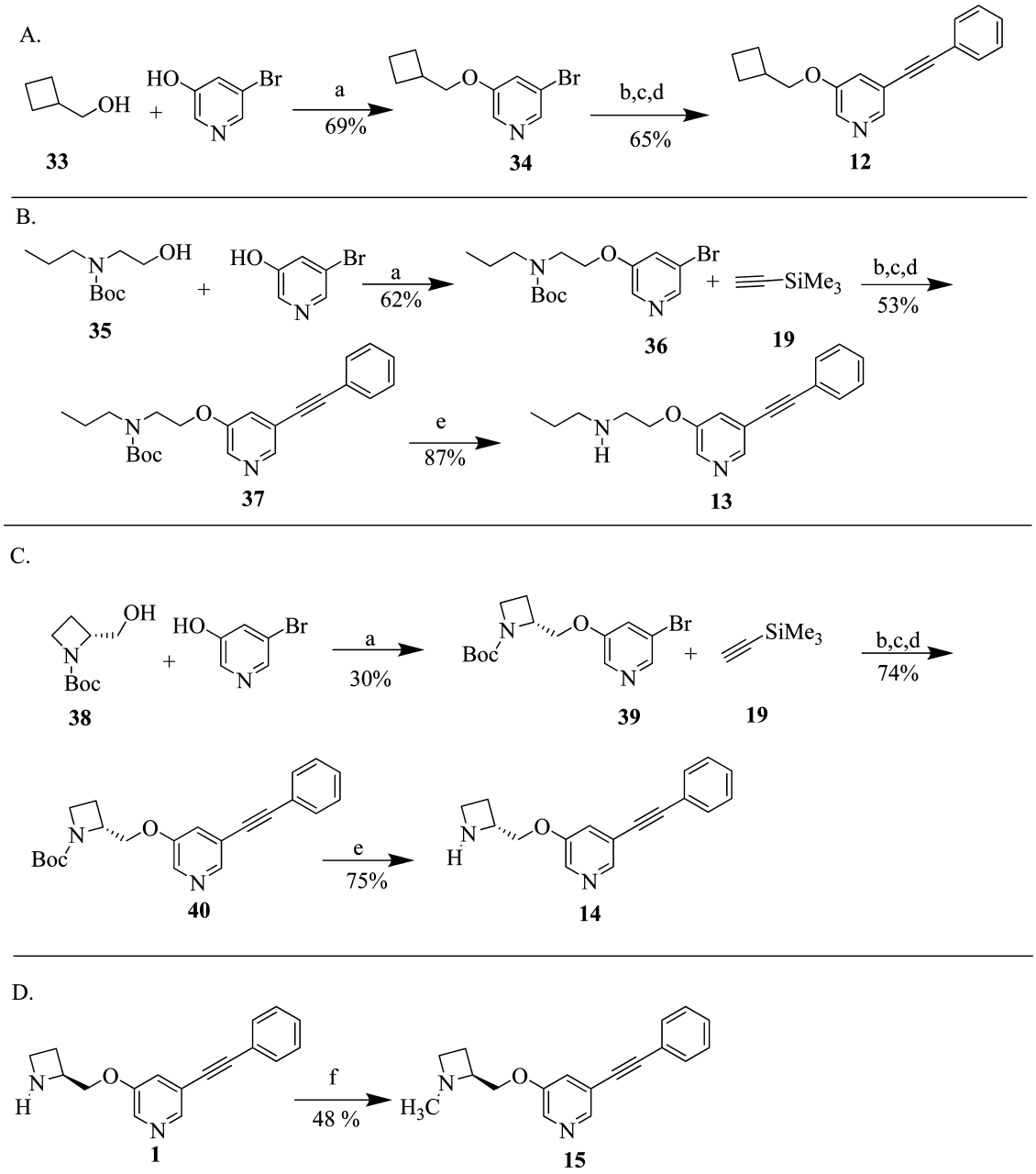

[a]Reagents and conditions: (a) DEAD, PPh_3, THF, 0 °C, 48 h; (b) 4 mol % $Pd(PPh_3)_2Cl_2$, 8 mol % PPh_3, 8 mol % CUI, iPr_2NH, toluene, 80 °C, 18 h; (c) KOH, MeOH/H_2O (4:1), 25 °C, 3 h; (d) iodobenzene, 25 °C, 16 h; (e) TFA, CH_2Cl_2, 0 °C−rt 4−6 h then 2 M NaoH in methanol in water (9:1), methanol, 18 h; (f) HCHO, $NaCNBH_3$, PH = 4−5 (CH_3COOH:CH_3COONa), ethanol.

Scheme 3. Synthesis of Compound 16[a]

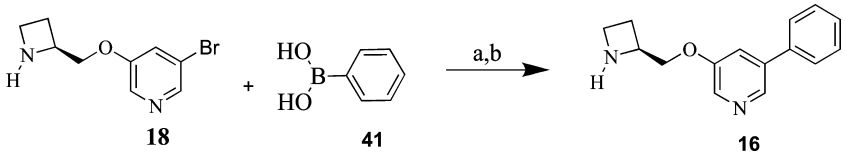

[a]Reagents and conditions: (a) $Pd(PPh_3)_4$, 2 M Na_2CO_3, toluene:ethanol (3:1), 90 °C, 18 h; (b) TFA, CH_2Cl_2, 0 °C−rt, 6 h then 2 M NaOH methanol in water (9:1), methanol, 18 h.

profile. In addition, the (*S*)-*N*-methyl compound **15** binds nearly 25 times weaker than the corresponding (*S*)-N−H compound **1**, suggesting that N−H provides a potentially important H-bond interaction. For comparing the difference between stereotypes, compound **14**, which is the (*R*)-form of compound **1**, was synthesized. The binding profile of **14** is

Table 1. Comparison of Binding Affinities of Series 1 Compounds for Rat nAChR Subtypes with Those of Saz-A, Varenicline, and Nicotine[a]

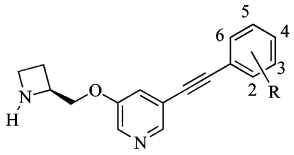

1 R=H
2, R=4-F
3 R=2-F
4 R=3-F
5 R= 3,5-F
6 R=3-CF_3
7 R=3-CH_3
8 R=3-Cl
9 R=3-$N(CH_3)_2$ and 5-F
10 R= 3-F and 5-CH_3
11 R= 3-F and 5-OCH_3

	K_i (nM)[b]								
compd ID	$\alpha2\beta2$	$\alpha2\beta4$	$\alpha3\beta2$	$\alpha3\beta4$	$\alpha4\beta2$	$\alpha4\beta4$	$\alpha7$	forebrain	$\alpha3\beta4/\alpha4\beta2$
1	0.11 (0.01)	58 (4)	0.53 (0.08)	640 (40)	0.049 (0.007)	11 (1)	580 (50)	0.5 (0.06)	13000
2	0.045 (0.016)	37 (7)	0.41 (0.09)	650 (20)	0.083 (0.029)	7.2 (0.7)	2,000 (800)	0.50 (0.05)	7800
3	0.081 (0.021)	47 (6)	0.61 (0.07)	580 (50)	0.072 (0.007)	8.7 (0.5)	1100 (500)	0.58 (0.10)	8100
4	0.029 (0.005)	31 (5)	0.19 (0.03)	520 (30)	0.032 (0.012)	5.3 (0.2)	720 (180)	0.44 (0.05)	16000
5	0.063 (0.011)	23 (1)	0.52 (0.34)	540 (60)	0.050 (0.009)	4.7 (0.6)	1,800 (700)	0.73 (0.05)	28000
6	0.28 (0.04)	54 (7)	1.4 (0.6)	1,400 (100)	0.26 (0.04)	11 (2)	1,300 (500)	3.5 (0.3)	5400
7	0.053 (0.004)	46 (4)	0.34 (0.14)	4,000 (2,900)	0.046 (0.011)	12 (3)	200 (80)	1.1 (0.4)	87000
8	0.19 (0.05)	150 (1)	1.6 (0.1)	3,400 (400)	0.093 (0.037)	17 (8)	480 (140)	1.7 (1.4)	37000
9	0.053 (0.012)	66 (3)	0.46 (0.22)	1,000 (30)	0.031 (0.003)	12 (2)	250 (93)	0.70 (0.37)	32000
10	0.064 (0.007)	38 (4)	0.24 (0.02)	1,100 (60)	0.043 (0.003)	8.1 (0.4)	590 (250)	1.4 (0.5)	26000
11	0.091 (0.011)	53 (2)	0.59 (0.01)	1,300 (40)	0.076 (0.017)	10 (0.3)	1,500 (100)	1.7 (0.3)	17000
Saz-A	0.087 (0.014)	210 (30)	0.38 (0.07)	1,900 (300)	0.062 (0.006)	52 (2)	670 (220)	0.17 (0.02)	31000
nicotine[c]	12 (2)	110 (20)	47 (11)	440 (60)	10 (2)	40 (6)	520 (140)	12 (2)	44
varenicline	0.22 (0.02)	71 (5)	1.9 (0.1)	460 (40)	0.13 (0.01)	15 (0.2)	62 (11)	0.71 (0.04)	3500

[a]Competition binding assays were carried out in membrane homogenates of stably transfected cells or rat forebrain tissue as described previously.[72−74] The rat nAChRs were labeled with [^{3}H]epibatidine. The K_d values for [^{3}H]epibatidine used for calculating K_i values were 0.02 for $\alpha2\beta2$, 0.08 for $\alpha2\beta4$, 0.03 for $\alpha3\beta2$, 0.3 for $\alpha3\beta4$, 0.04 for $\alpha4\beta2$, 0.09 for $\alpha4\beta4$, 1.8 for $\alpha7$, and 0.05 for rat forebrain. [b]K_i values of the compounds shown are the mean of 3−5 independent measurements with SEM values included in brackets. [c]The K_i values of (−)-nicotine was published previously.[72]

Table 2. Binding Affinities of Series 2 and Series 3 Compounds for Rat nAChR Subtypes[a]

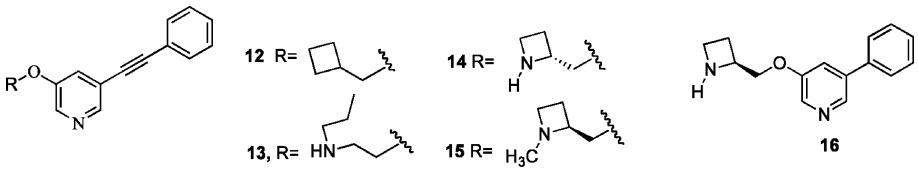

	K_i (nM)[b]								
compd ID	$\alpha2\beta2$	$\alpha2\beta4$	$\alpha3\beta2$	$\alpha3\beta4$	$\alpha4\beta2$	$\alpha4\beta4$	$\alpha7$	forebrain	$\alpha3\beta4/\alpha4\beta2$
12[c]	>100000	>50000	>25000	>1000000	>100000	>500000	>250000	>100000	
13[c]	>5000	>250000	>10000	>500000	>1000	>50000	>25000	>50000	
14	0.19 (0.05)	46 (16)	0.92 (0.26)	1700 (130)	0.11 (0.03)	8.9 (1.8)	1,600 (500)	1.1 (0.2)	15000
15	2.9 (0.5)	4,100 (400)	26 (2)	40,000 (4000)	1.2 (0.2)	1,100 (100)	7,700 (3000)	30 (2)	33000
16	0.22 (0.02)	36 (3)	5.0 (0.4)	1300 (200)	0.14 (0.01)	6.2 (0.3)	11,000 (3000)	1.1 (0.2)	9285

[a]Competition binding assays were carried out in membrane homogenates of stably transfected cells or rat forebrain tissue as described previously.[72−74] The rat nAChRs were labeled with [^{3}H]epibatidine. The K_d values for [^{3}H]epibatidine used for calculating K_i values were 0.02 for $\alpha2\beta2$, 0.08 for $\alpha2\beta4$, 0.03 for $\alpha3\beta2$, 0.3 for $\alpha3\beta4$, 0.04 for $\alpha4\beta2$, 0.09 for $\alpha4\beta4$, 1.8 for $\alpha7$, and 0.05 for forebrain. [b]K_i values of the compounds shown are the mean of 3−5 independent measurements with SEM values included in brackets. [c]The compound showed very low binding affinity at all nAChR subtypes. In the range of the concentration tested, no accurate K_i values could be determined. The numbers shown are estimated range of K_i values.

similar to that of compound **1**, although compound **14** has a slightly lower affinity for $\alpha4\beta2$ receptors than compound **1**. The binding affinity and drug-like properties of compound **1** prompted us to choose this molecule as a staring compound in the new series developed in this report and to advance this analogue in further in vitro and in vivo studies.

Binding Affinities for Targets Other than nAChRs. To determine the affinity of compound **1** to molecular targets other than neuronal nAChRs, 41 binding assays were evaluated including CNS receptors and transporters. As shown in the Supporting Information Table S1, the preliminary binding assays using a single concentration of compound **1** at 10 μM generated 32 "miss" (less than 50% inhibition of binding by specifically labeled ligands) and 9 "hit" (more than 50% inhibition of binding). The K_i values of compound **1** at these nine targets were determined by performing secondary binding assays using a series of concentrations of compound **1**. As shown in the Supporting Information Table S2, the compound has low binding affinities at these targets; thus, the binding

Table 3. Activation and Inhibition of nAChR Function by Compound 1, Saz-A, Varenicline, and Nicotine[a]

compd	α4β2 nAChRs[a]			α3β4 nAChRs[a]		
	EC_{50}[b] (nM)	E_{max}[c] (%)	$IC_{50(10')}$[d] (nM)	EC_{50} (nM)	E_{max} (%)	$IC_{50(10')}$ (nM)
1	10 ± 2	24 ± 3	16 ± 2	ND[e]	ND	>10000
sazetidine-A	24 ± 12	40 ± 2	11 ± 4	ND	ND	>10000
varenicline	950 ± 30	45 ± 2	94 ± 18	21,000 ± 1,000	82 ± 3	>10000
(−)-nicotine	2400 ± 300	100 ± 5	370 ± 110	24,000 ± 1,000	100 ± 2	>10000

[a]Functional properties of each compounds were determined in using stable cell lines expressing human α4β2 or rat α3β4 nAChRs. [b]EC_{50} values show potencies of agonist activities. [c]E_{max} values show relative efficacies of agonist activities, which were normalized to the E_{max} value of nicotine. [d]$IC_{50(10\ min)}$ values show potencies of desensitizer activities, which were determined by preincubated cells with various concentrations of test compounds for 10 min then exposed to 100 μM nicotine. [e]ND indicates no stimulation was detected. All values shown are means ± SEM of 3−9 independent experiments.

affinity of compound **1** for α4β2 nAChRs is at least 3000 times higher than that for any of those nine targets.

Molecular Modeling Interactions of Compound 1 and Other Known Ligands with the Agonist Form of the X-ray Crystal Structure of the AChBP. To better understand the binding interactions between α4β2 nAChR and compound **1**, molecular models of compound **1** with the α4β2 nAChR were constructed (Figure 2A) and overlaid with known nicotinic ligands (*S*)-nicotine, varenicline, and Saz-A (Figure 2B−D). The docked structural models of the α4β2 nAChR/ligand complex reveal that the binding mode interactions are slightly different from one another as reported previously.[37−43] To provide a consistent model with the nicotine-AChBP (PDB: 1UW6), the docked position of each compound was remodeled using a step-by-step manual docking methodology with restrained molecular dynamic (MD) simulations followed by energy minimization. In the restrained MD simulations, the optimum van der Waals and H-bond distance constraints was set between the ligand and the α4β2 nAChR ligand binding domain residues. The final binding complex is depicted in Figure 2A−D.

The compound **1**, nicotine, varenicline, and Saz-A are predicted to be buried near aromatic rich residues such as W147α, W55β, Y91α, Y188α, Y195α, and F117β (Figure 2A−D) and are expected to occupy a similar binding region. However, MD simulations suggest a slightly different orientation of the compounds in the α4β2 binding site. This may be due to conformational adjustments inside the binding site. The azetidine group in compound **1** and Saz-A are shown forming stacking interactions with the amino acid W147α (Figure 2A,D). However, positioning of the pyridine group is slightly perturbed to compensate for the conformational entropy penalty due to isomeric constraints. The hydroxy group of Saz-A may form a hydrogen bond with Y188α, whereas this residue likely forms a hydrogen bond with the pyrazine ring nitrogen of varenicline, and this hydrogen bond is absent in (*S*)-nicotine. Compound **1** and Saz-A have hydrophobic groups extending from the pyridine ring, which may form additional favorable hydrophobic interactions with K76β, K77β, Y112β, V109β, F117β, and L119β. These interactions can be compared with the interactions of varenicline involving V109β, F117β, and L119β (Figure 2C). Although Saz-A and compound **1** are shown to have a similar pattern of interaction, the benzene ring of the ethynylbenzene of compound **1** can form a stronger stacking and lipophilic interaction with K76β, K77β, Y112β, and V109β than the corresponding hex-5-yn-1-ol group of Saz-A. Moreover, the 3-(2-phenylethynyl) pyridine group of compound **1** is more rigid and may require a smaller penalty in conformational entropy as compared to the flexible 6-(3-pyridyl) hex-5-yn-1-ol group of Saz-A (Figure 2A,B). These additional interactions and favorable entropy penalty may likely confer potency to compound **1**. The overlay of compound **1** with (*S*)-nicotine, varenicline, and Saz-A (Figure 2B−D) suggests that compound **1** forms more favorable hydrophobic interactions with the α4β2 nAChR and occupies different receptor space that may be critical for selective and high affinity binding.

Effects of Compound 1 on Functions of nAChRs. The functional effect of the lead compound **1** was assessed by measuring agonist-stimulated $^{86}Rb^+$ efflux from stably transfected cells expressing nAChRs, either human α4β2 subtype or rat α3β4 subtype. Its ability to desensitize nAChRs was determined by measuring nicotine-stimulated $^{86}Rb^+$ efflux after cells were preincubated with compound **1** for 10 min. For comparison, we also examined three other nicotinic ligands in the same manner, Saz-A, varenicline, and (−)-nicotine.

As shown in Table 3, compound **1** did not show any detectable agonist activity at rat α3β4 nAChRs in $^{86}Rb^+$ efflux assays. At human α4β2 receptors, the compound showed agonist activity with an EC_{50} value as 10 nM and a maximal efficacy (E_{max}) relative to the maximal stimulation by nicotine of 24%. In parallel experiments, varenicline also showed partial agonist activity at α4β2 receptors (45%) and, at much higher concentrations, near-full agonist activity at α3β4 nAChRs (85%). The full activation and desensitization curves of compound **1** are shown in Supporting Information Figure S1.

It is important to note that all four compounds studied, compound **1**, Saz-A, varenicline, and nicotine inhibited nicotine activation of α4β2 receptors after preincubation with the cells for 10 min, which desensitizes the receptors. As shown in Table 3, after a 10 min preincubation, compound **1** potently desensitized α4β2 receptor function with an IC_{50} value ($IC_{50(10'')}$) of 16 nM, indicating a potency for desensitization of these receptors similar to that of Saz-A, but 6- and 23-times more potent than varenicline and nicotine, respectively. In contrast to their high potency to desensitize α4β2 nAChRs, the $IC_{50(10'')}$ values of these four compounds to desensitize α3β4 nAChRs were greater than 10000 nM (Table 3). All of these compounds, especially compound **1** and Saz-A, are much more potent desensitizers of α4β2 than α3β4 nAChRs.

To confirm that compound **1** is a low efficacy agonist of α4β2 nAChRs, we evaluated the compound for its agonist activity at α4β2 nAChRs using whole cell patch clamp. In all cells studied ($n = 3$), the bath application of compound **1** (200 nM) produced a mean inward whole-cell current that was 12.61 ± 1.8% of the control whole-cell response to 32 μM ACh. This electrophysiological study confirms that compound **1** has very low agonist efficacy for α4β2 nAChRs.

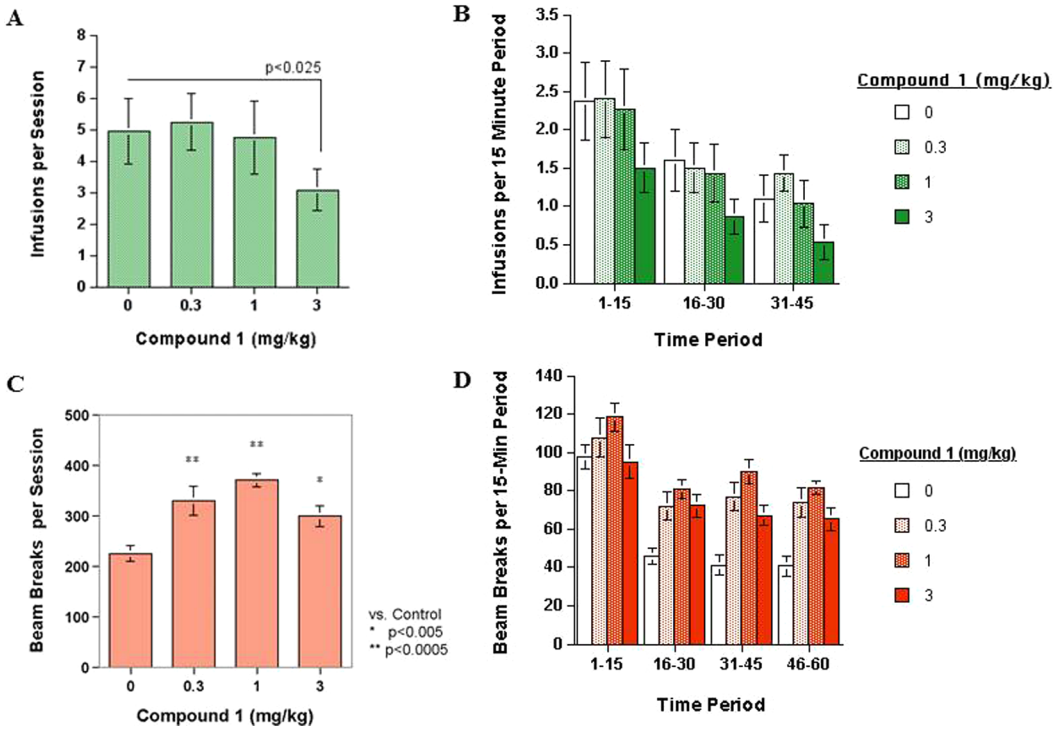

Figure 3. (A) Acute compound **1** effects on nicotine self-administration (0.03 mg/kg/infusion). Compound **1** (3 mg/kg) resulted in a significant ($p < 0.025$) decrease in nicotine self-administration relative to nicotine self-administration after control saline injections (mean ± SEM; $n = 15$). (B) Compound **1** effects on nicotine self-administration during each 15 min time period within session. (C) Acute compound **1** effects on locomotor activity. Effect of compound **1** on locomotor activity in the figure-eight maze during the 1 h session (mean + SEM; $n = 12$). (D) Compound **1** effects on locomotor activity during each 15 min time period within session.

Table 4. Calculated Ligand Efficiency and Physicochemical Properties of Compounds in Series 1

	binding affinity K_i (nM)	ligand efficiency kcal/mol	predicted physicochemical properties			
compd ID	$\alpha4\beta2$	LE[a]	MW[b]	CLogP[b]	PSA[c]	log BB[d]
1	0.049	0.70	264.32	3.712	34.15	0.2
2	0.083	0.65	282.31	3.855	34.15	0.22
3	0.072	0.66	282.31	3.855	34.15	0.22
4	0.032	0.68	282.31	3.855	34.15	0.22
5	0.050	0.64	300.30	3.998	34.15	0.24
6	0.26	0.54	332.32	4.595	34.15	0.33
7	0.046	0.67	278.35	4.211	34.15	0.27
8	0.093	0.65	298.77	4.425	34.15	0.30
9	0.031	0.60	325.38	4.191	37.39	0.22
10	0.043	0.64	296.34	4.354	34.15	0.29
11	0.076	0.60	312.34	3.914	43.38	0.1
Saz-A	0.062	0.73	260.33	1.47	54.38	−0.44
varenecline	0.12	0.85	211.26	0.899	37.81	−0.28
nicotine	10	1.14	162.23	0.883	16.13	−0.035

[a]Ligand binding efficiency was calculated according to the Hopkins equation: LE = 1.372 × (−log K_i (moles))/N. [b]Molecular weight and cLogP were calculated from ChemBioDraw Ultra 11.0. [c]Polar surface area (PSA) was calculated from www.chemicalize.org. [d]Log BB was calculated from the following equation: Log BB = −0.0148PSA + 0.152CLogP + 0.139.

Effects of Compound 1 on Nicotine Self-Administration and Locomotor Activity in Rats. The lever press data from the 10 training sessions clearly shows that the nicotine lever is preferred (active lever 12.6 ± 1.2 presses/session, inactive lever 3.2 ± 0.3 presses per session, ($F(1,14) = 28.55$, $p < 0.0005$) and that it is stable over this period. We then studied acute effects of compound **1** on nicotine self-administration in rats. As shown in Figure 3A, compound **1** significantly ($F(3,42) = 3.36$, $p < 0.05$) decreased intravenous nicotine self-administration. The 3 mg/kg dose of compound **1**, but not the lower doses, caused a significant ($p < 0.025$) decrease in the number of nicotine infusions compared with vehicle. The 15 min time periods within each session were analyzed (Figure 3B). There was a significant ($F(2,28) = 19.85$, $p < 0.0005$) main effect of time period reflecting the commonly seen initial higher rate of nicotine self-administration during each session. However, there was no significant interaction of compound **1** multiplied by time period within session. The effect of repeated dosing was also analyzed. The entire range of compound **1** doses and the saline control were given twice.

A.

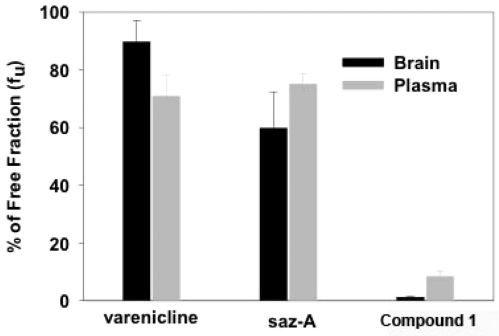

B.

Compound	Free Fraction Percentage of Drug in Plasma Protein ($f_{u,\ protein}$)	Free Fraction Percentage of Drug in Brain Tissue Homogenate ($f_{u,\ brain}$)
1	8.40 ± 1.8	1.21 ± 0.2
Saz-A	75.1 ± 3.7	59.8 ± 12.6
Varenicline	70.9 ± 7.4	89.7 ± 7.4
Propranolol	9.61	-
Haloperidol	-	1.60

Figure 4. Unbound fraction of each compound in the rat brain tissue and plasma protein using an equilibrium dialysis method. (A) Representative percentage of free fraction of rat plasma and brain tissue against each compound tested at 5 μM for 4 h. (B) Representative data summary of free fractions of the brain tissue and plasma protein against each compound.

There was no significant effect of the repeated testing and no significant interaction compound **1** with repeated dosing. These data demonstrate that, similar to Saz-A,[26] compound **1** at 3 mg/kg effectively reduces nicotine self-administration in rats.

Interestingly, the locomotor activity of rats was significantly increased by compound **1** ($F(3,33) = 13.58$, $p < 0.0005$). All three doses of compound **1** significantly ($p < 0.0005$ for 0.3 and 1 mg/kg and $p < 0.005$ for 3 mg/kg) increased the mean activity over the 1 h test session (Figure 3C). Therefore, the effect of compound **1** in decreasing nicotine self-administration did not appear to result from any drug induced sedative effect. Furthermore, the dose−effect function of compound **1** on locomotor activity did not correspond with the effect on nicotine self-administration, as the peak of increased locomotor activity was at 1 mg/kg, at which dose there was no significant reduction of nicotine self-administration. There was a significant main effect of 15 min time blocks within the session ($F(3,33) = 79.68$, $p < 0.0005$), reflecting the normal habituation of locomotor exploration (Figure 3D), but the drug treatment multiplied by the block interaction was not significant.

Physicochemical Properties of the New Ligands. Several key physicochemical properties of compounds may influence the blood−brain barrier (BBB) penetration of CNS drugs,[44,45] including molecular weight (MW), polar surface area (PSA), and lipophilicity (clogP). These parameters were calculated for all series 1 compounds and are presented in Table 4. In general, CNS drugs have a MW ≤ 450 Da. All the compounds in this report have molecular weights less than 450 Da. In addition, all these compounds have clogP values <5, suggesting a reasonable probability of good oral absorption and intestinal permeability.[46] In general, a polar surface area (PSA) less than 60 Å^2 is predictive of good penetration of the blood−brain barrier. As shown in Table 4, all the compounds in series 1 have PSA values less than than 60 Å^2. We also calculated the log BB, which is a parameter commonly used to express the extent of a drug passing through the blood−brain barrier.[47] Several QSAR models were developed to calculate the log BB.[48] In this study, we used Clark's equation to predict the log BB values for compounds in series 1.[49] In general, a log BB value greater than zero is a favorable factor for BBB penetration. The log BB values of all compounds in series 1 were in the positive range. Ligand efficiency (LE) is an important metric in drug discovery and has been used to measure the relationship of a ligand's affinity with molecular size. LE is the ratio of the free energy of binding over the number of heavy atoms in a molecule.[50] LE is a useful optimization tool to evaluate a ligand's ability to effectively bind to the targeted protein. Considering the binding affinity (K_i) of the compounds in series 1, we calculated the LE using Hopkin's equation.[51] An LE ≥ 0.3 is considered favorable and suggests that a compound is optimized for receptor occupancy. All compounds in series 1 have an LE value in the range of 0.6 to 1 kcal/mol (Table 4).

Brain Tissue Distribution and Plasma Binding Studies for Compound 1. To study in vitro unbound brain-to-plasma concentration ratio of compound **1**, we applied an equilibrium dialysis technique as described in the Experimental Procedures. As shown in Figure 4A,B, compound **1** (5 μM) has a significantly less percentage of unbound drug fraction in the rat brain tissue ($\%f_{UBrain} = 1.21$) as compared to Saz-A ($\%f_{UBrain} = 59.8$) and varenicline ($\%f_{UBrain} = 89.7$). We also found that the observed percentage of unbound drug fraction in plasma protein for compound 1 ($\%f_{Uplasma} = 8.40$) is higher than that of brain tissue (Figure 4A,B). These results support that compound 1 may have better brain tissue distribution as compared to Saz-A.

■ DISCUSSION AND CONCLUSIONS

Tobacco use and nicotine addiction imposes a huge health and economic burden. Cytisine, a plant alkaloid, has been used for aiding smoking cession in Eastern and Central European countries since 1964.[52] To date, there are only three classes of medications that have been approved by the U.S. Food and Drug Administration for smoking cessation: nicotine replacement therapy, bupropion, and varenicline. Among the three,

varenicline, which is a rational designed compound related to cytisine, is considered superior in terms of relative efficacy over a period of 3 months, at which time ∼44% of the subjects were abstinent. However, the percentage of subjects who remained smoke-free for 12 months following treatment with varenicline fell to ∼22%.[17,18] Moreover, although varenicline appears to be safe for most people, exacerbation of schizophrenia and manic episodes associated with treatment with varenicline has been reported.[53,54] In addition, based on a very recent report,[55] the FDA issued a "notification" warning that varenicline may be associated with increased adverse cardiovascular events, including angina and heart attack. More commonly, nearly 30% of participants taking varenicline in clinical trials reported nausea and 18% reported vomiting.[17,18]

Although varenicline was developed as a partial agonist at $\alpha4\beta2$ nAChRs,[56] it is also nearly a full agonist at $\alpha3\beta4$ nAChRs, which predominate in autonomic ganglia and brainstem autonomic centers, as well as at $\alpha7$ nAChRs, another important subtype in brain.[23] However, it is not known if varenicline reaches concentrations necessary to act at these receptors. More recently, varenicline was found to be a potent agonist of the human 5-hydroxytryptamine$_3$ receptors (5-HT$_3$).[57] The side effects of varenicline are most likely mediated through its actions at receptors other than $\alpha4\beta2$* nAChRs, including $\alpha3\beta4$* and/or $\alpha7$ nAChRS and/or 5-HT$_3$ receptors.

Given the grave health and economic consequences of smoking, there is an obvious great need for significant improvement in the existing smoking cessation therapies. On the basis of a study of Saz-A, which desensitizes $\alpha4\beta2$ nAChRs potently and with high selectivity, we previously proposed a strategy to develop novel nicotinic therapeutic drugs, including smoking cessation drugs, based on their ability to selectively desensitize $\alpha4\beta2$ nAChRs.[25]

The high potency of Saz-A to desensitize $\alpha4\beta2$ nAChRs in cells in vitro suggested that it would produce important effects similar to some of those produced by nicotine but with much more receptor selectivity. It would therefore potentially be a drug candidate to help people overcome addiction to nicotine, as well as to treat other CNS disorders. Since 2007, Saz-A studies in rodents have found that it reduces nicotine self-administration[28,58] and alcohol intake[29] and produces anti-nociceptive effects[59,60] and preclinical effects consistent with anxiolytic[32] and possible antidepressant activity.[31,33,61] Interestingly, it also increased attention and reduced errors in rats even after pretreatment with scopolamine and dizocilpine, drugs that normally disrupt attention.[30]

Recent studies found that the Saz-A reached only low concentrations in brain, even after chronic administration.[33,34] Compound **1** emerged from an effort to improve brain penetration of drugs that could selectively target $\alpha4\beta2$ nAChRs. Thus, while the synthesis and structure of compound **1** are based on the Saz-A scaffold, its physiochemical properties, especially its PSA and clogP, favor improved entry into the brain. The binding model of $\alpha4\beta2$ nAChR with compound **1** suggests similar occupancy of the binding pocket as that of nicotine and varenicline. Moreover, the phenylethynyl group at the C-5 position of the pyridine in compound **1** occupies a potentially critical space in the pocket to form favorable hydrophobic interactions with the receptor (Figure 2A).

In binding studies, compound **1** and analogues (Scheme 1) are highly selective for $\alpha4\beta2$ nAChRs over $\alpha3\beta4$ and $\alpha7$ subtypes (Table 1). In studies of receptor function as assessed in $^{86}Rb^+$ efflux assays, compound **1** has less than 30% of the efficacy of nicotine in activating human $\alpha4\beta2$ nAChRs (Table 3). Importantly, the potency of compound **1** to desensitize $\alpha4\beta2$ nAChRs is similar to that of Saz-A and much more potent than varenicline or nicotine (Table 3).

Consistent with an excellent pharmacological property profile, improved physicochemical properties and brain tissue distribution (Figure 4), compound **1** significantly reduced nicotine self-administration in the rat model (Figure 3). This suggests that compound **1** has the potential to be developed into a smoking cessation drug.

There were differences between the effects of compound **1** and Saz-A on locomotor activity. Compound **1** caused a modest but significant increase in locomotor exploration in the figure-eight apparatus at all three doses tested (1−3 mg/kg). In contrast, in the same test, Saz-A did not show any apparent effect on locomotor activity at 1 and 3 mg/kg (Saz-A produced a slight decrease in activity at the beginning of the test session). Compound **1** may have less risk of sedative side effects than Saz-A.

To elucidate SAR for compound **1**, in addition to compounds in series 1 (compounds **1**−**11**), we also synthesized four compounds in series 2, including **12**, **13**, **14**, and **15** (Scheme 2A−D). The very low binding affinities of compounds **12** and **13** may be an indication that the azetidine ring is important for good binding property profiles. The binding affinity of (*S*)-*N*-methyl compound **15** is 25 times lower than that of corresponding (*S*)-N−H compound **1**. It is conceivable that the N−H provides a potentially important H-bond interaction. It is interesting that the two enantiomers, compound **14** and compound **1**, showed a similar binding profile although compound **14** has a slightly lower affinity for $\alpha4\beta2$ receptors than compound **1**. In series 3, we replaced the alkyne group and made a direct link to pyridine as shown in compound **16** (scheme 3). The binding data suggested that a spacer is necessary to retain activity similar to that of compound **1**.

It is important to note that all binding data in this study are from rat nAChRs, as well as functional data for $\alpha3\beta4$ receptor subtype. Rat nAChRs were instrumental in the discovery of clinically used nicotinic drugs. In the consideration of possible species difference, we are currently studying these novel compounds using human nAChR subtypes. We will report the comparative results once the study is completed.

In screening studies, compound **1** did not show high binding affinity for more than 40 other CNS receptors (Tables S1 and S2, Supporting Information), including 5-HT$_3$ receptors, which could mediate some of varenicline's adverse side effects, including nausea.[56]

In summary, genetic and pharmacological studies suggest that $\alpha4\beta2$ nAChRs are crucial to nicotine self-administration in rodents and likely very important in nicotine addiction. Developing novel drug candidates that selectively target the $\alpha4\beta2$ nAChR subtype may provide an important therapeutic advance for treating nicotinic addiction/dependence. Compound **1** represents the lead of a class of novel compounds that maintain the excellent pharmacological profile of Saz-A but with improved physicochemical properties.

■ EXPERIMENTAL PROCEDURES

Chemistry. All reagents and solvents used in this study were commercially available and used as obtained. Purification of compounds was performed by chromatography using a Biotage SP-1 system with silica gel cartridges. NMR spectra were recorded on a

Varian 400 MR spectrometer at 400 MHz for ^{1}H and 100 MHz for ^{13}C. Chemical shifts (δ) are expressed in ppm downfield from tetramethylsilane, and coupling constants (**J**-values) are reported in hertz (Hz). Molecular mass spectra measured using a Waters Q-TOF premier mass spectrometer. The purity of final compounds was evaluated by C, H, N analysis (Atlantic microlabs) and HPLC methods for compounds **9** and **15** (Figure S2, Supporting Information). The purities of all the final compounds were confirmed to be ≥95% by combustion and HPLC analytical methods. The HPLC method of purity (**9** and **15**) was confirmed using two different mobile phases as described in the Supporting Information (Figure S2). Detailed synthetic and characterization data of intermediate compound 3-fluoro-5-iodo-*N*,*N*-dimethylaniline (VMY-2-119) was presented in Supporting Information experimental procedures.

General Procedure for the Mitsunobu Reaction (18). To a mixture of 5-bromo-3-pyridinol (1.2 equiv) and Ph_3P (1.6 equiv) in anhydrous THF taken in a flame-dried flask under N_2, *N*-Boc protected alcohol (1 equiv) was added and the mixture was cooled to −10 °C. Diethyl azodicarboxylate (40% w/v) in toluene (1.6 equiv) was added dropwise to the mixture and was warmed gradually to the room temperature. After 48 h, the reaction mixture was quenched with 1 mL of water and the solvent was removed under reduced pressure. The resulting yellow oil was purified by column chromatography on silica gel to yield 55−60% as the white solid.

General Procedure for Sonogashira Coupling Reaction. *Sequential Desilylation and Sonogashira Coupling of the TMS Protection (**22**−**25**).* Route 1 in Scheme 1: An oven-dried and nitrogen-filled round-bottom flask was charged with (*S*)-*tert*-butyl-2-((5-((trimethylsilyl)ethynyl)pyridin-3-yloxy)methyl)azetidine-1 carboxylate (**20**, 1 equiv), KOH (2 equiv) methanol in water (20:1). The whole reaction mixture was stirred 25 °C for 3 h. It was then added to a second flask, which contained a performed mixture of $Pd(PPh_3)_2Cl_2$ (0.02 equiv, 2 mol %), CuI (0.02 equiv, 2 mol %), PPh_3 (0.04 equiv, 4 mol %), i-Pr_2NH (1 mL), toluene (3−5 mL), and substituted fluoro-iodobenzene that had been prestirred at 25 °C for 30 min. The complete mixture was then stirred at 25 °C for 16 h. The reaction mixture was quenched with a saturated NH_4Cl solution and extracted with CH_2Cl_2. The combined organic layers were washed with 2N HCl, water, and saturated NaCl solution. The organic phase was separated and dried over anhydrous sodium sulfate, filtered, and concentrated under reduced pressure to give crude product. The crude product was purified by column chromatography.

*One-Pot Synthesis (**22**, **26**−**32**).* Route 2 in Scheme 1: The Mitsunobu adduct (**18**, 1 equiv), $Pd(PPh_3)_2Cl_2$ (0.04 equiv, 4 mol %), CuI (0.08 equiv, 8 mol %), and PPh_3 (0.08 equiv, 8 mol %) were placed in a oven-dried round-bottom flask with nitrogen. After addition of i-Pr_2NH (1 mL) and toluene (3−5 mL), the mixture was stirred at room temperature for 5 min and (trimethylsilyl) acetylene (**19**, 2.7 equiv) was added and stirred at rt for 10 min. The whole reaction mixture was stirred at 80 °C for 18 h, a solution of KOH in methanol and water (4:1) was added in one portion, and the mixture was stirred for additional 3 h at 25 °C. A second substituted aryl iodide was added and stirred continually for 16 h at 25 °C (80 °C in case of substituted aryl bromide). The reaction mixture was quenched with saturated NH_4Cl solution and extracted with CH_2Cl_2. The combined organic layers were washed with 2 N HCl, water, and saturated NaCl solution. The organic phase was separated and dried over anhydrous sodium sulfate, filtered, and concentrated under reduced pressure to give the crude product. The crude product was purified by column chromatography.

General Procedure for the Deprotection of the N-Boc Precursors. Route 1, method e, and route 2, method i: To a stirred solution of *N*-Boc protected compound in dichloromethane was added trifluoro acetic acid (5−10 equiv) dropwise at 0 °C under a nitrogen atmosphere. The reaction mixture was stirred at room temperature for 4−6 h (TLC showed complete deprotection of Boc after 5 h). The solvent and excess of TFA was removed under reduced pressure. The resulting residue was further apply the nitrogen to remove the traces of TFA and was taken in 2−3 mL methanol followed by dropwise addition 2 M NaOH solution in methanol and water (9:1) at 0 °C until the pH 9−10. The reaction mixture stirred for 18 h, upon which dichloromethane (10−20 mL) was added and rotary evaporated. The resulting residue was purified by column chromatography.

*(S)-3-(Azetidin-2-ylmethoxy)-5-(phenylethynyl)pyridine (**1**).* Route 2 (method i) in Scheme 1 was used and generated a yield of 70% (liquid). ^{1}H NMR (400 MHz, $CDCl_3$): δ 8.37 (s, 1H), 8.31−8.25 (m, 1H), 7.60−7.49 (m, 2H), 7.41−7.29 (m, 4H), 4.33−4.20 (m, 1H), 4.10−3.96 (m, 2H), 3.69 (q, *J* = 7.9, 1H), 3.45 (td, *J* = 4.8, 8.1, 1H), 2.45−2.19 (m, 3H). ^{13}C NMR (100 MHz, $CDCl_3$): δ 154.4, 144.5, 137.7, 131.6, 128.7, 128.4, 122.9, 122.4, 120.4, 92.3, 85.8, 72.7, 56.9, 44.2, 23.9. HRMS (ESI): exact mass calcd for $C_{17}H_{16}N_2O$ [M + H]$^+$, 265.1341; found, 265.1339. $[\alpha]_D^{23.4}$ = −6.0 (*c* = 1.1, $CHCl_3$). Anal. Calcd for $C_{17}H_{16}N_2O$: C,77.25; H, 6.10; N, 10.60. Found: C, 77.22; H, 6.13; N, 10.51.

*(S)-3-(Azetidin-2-ylmethoxy)-5-((4-fluorophenyl)ethynyl)pyridine (**2**).* Route 1 (method e) in Scheme 1 was used and generated a yield of 77% (liquid). ^{1}H NMR (400 MHz, $CDCl_3$): δ 8.27 (s, 1H), 8.19 (d, *J* = 2.8, 1H), 7.47−7.39 (m, 2H), 7.23 (dd, *J* = 1.5, 2.7, 1H),7.00−6.93 (m, 2H), 4.20 (s, 1H), 4.04−3.90 (m, 2H), 3.62 (d, *J* = 7.2, 1H), 3.37 (s, 1H), 2.37−2.14 (m, 3H). ^{13}C NMR (100 MHz, $CDCl_3$): δ 162.7 (d, J_{F-C} = 249 Hz, C), 154.4, 144.5, 137.8,133.6 (d, J_{F-C} = 8.5), 122.8, 120.3, 118.6 (d, J_{F-C} = 3.5), 115.7 (d, J_{F-C} = 23 Hz), 91.2, 85.6, 72.8, 57.0, 44.2, 23.9. HRMS (ESI): exact mass calcd for $C_{17}H_{15}FN_2O$ [M + H]$^+$, 283.1247; found, 283.1241. $[\alpha]_D^{24.4}$ = −6.1 (*c* = 0.54, $CHCl_3$) . Anal. Calcd for $C_{17}H_{15}FN_2O{\cdot}0.1H_2O$: C, 71.63; H, 5.41; N, 9.82. Found: C, 71.21; H, 5.41; N, 9.76

*(S)-3-(Azetidin-2-ylmethoxy)-5-((2-fluorophenyl)ethynyl)pyridine (**3**).* Route 1 (method e) in Scheme 1 was used and generated a yield of 81% (liquid). ^{1}H NMR (400 MHz, $CDCl_3$): δ 8.31 (d, *J* = 1.0, 1H), 8.21 (dd, *J* = 2.7, 0.9, 1H), 7.49−7.41 (m, 1H), 7.31−7.23 (m, 2H), 7.11−7.00 (m, 2H), 4.29−4.14 (m, 1H), 4.05−3.91 (m, 2H), 3.63 (q, *J* = 7.9, 1H), 3.39 (td, *J* = 7.8, 5.0, 1H), 2.41−2.11 (m, 3H). ^{13}C NMR (100 MHz, $CDCl_3$): δ 162.5 (d, J_{F-C} = 251 Hz), 154.4, 144.5, 138.1, 133.3 (d, J_{F-C} = 1.0), 130.5 (d, J_{F-C} = 8.0), 124.0 (d, J_{F-C} = 3.7), 122.8, 120.0, 115.5 (d, J_{F-C} =21 Hz), 111.0(d, J_{F-C} =16 Hz), 90.7 (d, J_{F-C} = 3.3), 85.6, 72.7, 56.9, 44.1, 23.8. HRMS (ESI): exact mass calcd for $C_{17}H_{15}FN_2O$ [M + H]$^+$, 283.1247; found. 283.1243. $[\alpha]_D^{24.7}$ = −11.5 (*c* = 0.87, $CHCl_3$). Anal. Calcd for $C_{17}H_{15}FN_2O$: C, 72.32; H, 5.36; N, 9.92. Found: C, 71.82; H, 5.38; N, 9.77.

*(S)-3-(Azetidin-2-ylmethoxy)-5-((3-fluorophenyl)ethynyl)pyridine (**4**).* Route 1 (method e) in Scheme 1 was used and generated a yield of 78% (liquid). ^{1}H NMR (399 MHz, $CDCl_3$): δ 8.30 (d, *J* = 1.6, 1H), 8.22 (d, *J* = 2.8, 1H), 7.30−7.23 (m, 3H), 7.20−7.13 (m, 1H), 7.07−6.95 (m, 1H), 4.29−4.15 (m, 1H), 3.98 (qd, *J* = 9.5, 5.5, 2H), 3.65 (q, *J* = 7.9, 1H), 3.46−3.35 (m, 1H), 2.42−2.13 (m, 3H). ^{13}C NMR (100 MHz, $CDCl_3$): δ 162.3 (d, J_{F-C} = 246 Hz). 154.4, 144.6, 138.0, 130.0 (d, J_{F-C} =9 Hz), 127.5 (d, J_{F-C} = 3.1 Hz), 124.2 (d, J_{F-C} = 9 Hz), 123.0, 120.0, 118.4 (d, J_{F-C} =23 Hz), 116.1(d, J_{F-C} =21 Hz), 116.0, 90.9 (d, J_{F-C} = 3.4), 72.8, 57.0, 44.2, 23.9. HRMS (ESI): exact mass calcd for $C_{17}H_{15}FN_2O$ [M + H]$^+$, 283.1247; found, 283.1236. $[\alpha]_D^{24.8}$= −8.4 (*c* = 0.8, $CHCl_3$). Anal. Calcd for $C_{17}H_{15}FN_2O$: C, 72.32; H, 5.36; N, 9.92. Found: C, 72.03; H, 5.46; N, 9.78

*(S)-3-(Azetidin-2-ylmethoxy)-5-((3,5-difluorophenyl)ethynyl)-pyridine (**5**).* Route 2 (method i) in Scheme 1 was used and generated a yield of 79% (liquid). ^{1}H NMR (400 MHz, $CDCl_3$): δ 8.29 (d, *J* = 1.6,1H), 8.24 (d, *J* = 2.8, 1H), 7.25 (dd, *J* = 1.7, 2.8, 1H), 7.03−6.94 (m, 2H), 6.77 (tt, *J* = 2.3, 8.9, 1H), 4.23 (s, 1H), 3.99 (qd, *J* = 5.5, 9.5, 2H), 3.66 (d, *J* = 7.6, 1H), 3.39 (s, 1H), 2.48−1.79 (m, 3H).^{13}CNMR (100 MHz, $CDCl_3$): δ 163.9 (d, J_{F-C} = 13 Hz), 161.4 (d, J_{F-C} =13 Hz), 154.4, 144.6, 138.4, 125.1(t), 123.0, 119.5, 114.7 (d, J_{F-C} = 8 Hz), 114.5 (d, J_{F-C} = 7.7), 104.9 (t), 89.8 (t, J_{F-C} = 3.9), 87.7, 72.9, 56.9, 44.2, 23.9. HRMS (ESI): exact mass calcd for $C_{17}H_{14}F_2N_2O$ [M + H]$^+$, 301.1152; found, 301.1155. $[\alpha]_D^{24.5}$= −8.0 (*c* = 0.8, $CHCl_3$). Anal. Calcd for $C_{17}H_{14}F_2N_2O{\cdot}0.06H_2O$: C, 67.74; H, 4.72; N, 9.28. Found: C, 67.35; H, 4.68; N, 9.10.

*(S)-3-(Azetidin-2-ylmethoxy)-5-((3-(trifluoromethyl)phenyl)-ethynyl)pyridine (**6**).* Route 2 (method i) in Scheme 1 was used and generated a yield of 78% (liquid). ^{1}H NMR (400 MHz, $CDCl_3$): δ 8.31 (d, *J* = 1.6, 1H), 8.24 (d, *J* = 2.8, 1H), 7.74 (s, 1H), 7.64 (d, *J* = 7.7, 1H), 7.55 (d, *J* = 7.9, 1H), 7.43 (t, *J* = 7.8, 1H), 7.27 (dd, *J* = 1.7,

2.8, 1H), 4.23 (td, J = 7.5, 12.3, 1H), 3.99 (qd, J = 5.5, 9.5, 2H), 3.66 (dd, J = 8.1, 15.9, 1H), 3.40 (dt, J = 4.9, 7.6, 1H), 2.52−1.90 (m, 3H). ^{13}C NMR (100 MHz, $CDCl_3$): δ 154.4, 144.6, 138.2, 134.6 (d, J = 1.1), 131.0 (q), 128.9, 128.4 (d, J = 3 Hz), 125.2 (d, J = 3.7), 123.4, 123.0, 119.8, 90.6, 87.3, 72.8, 57.0, 44.2, 23.9. HRMS (ESI): exact mass calcd for $C_{18}H_{15}F_3N_2O$ [M + H]$^+$, 333.1215; found, 333.1216. $[\alpha]_D^{24.7}$ = −7.8 (c = 4.2, $CHCl_3$). Anal. Calcd for $C_{18}H_{15}F_3N_2O$: C, 65.06; H, 4.55; N, 8.43. Found: C, 64.74; H, 4.45; N, 8.30.

*S)-3-(Azetidin-2-ylmethoxy)-5-(m-tolylethynyl)pyridine (**7**).* Route 2 (method i) in Scheme 1 was used and generated a yield of 68% (liquid). ^{1}H NMR (400 MHz, $CDCl_3$): δ 8.26 (t, J = 2.9, 1H), 8.17 (d, J = 2.8, 1H), 7.30−7.21 (m, 3H), 7.15 (t, J = 7.6, 1H), 7.10−7.05 (m, 1H), 4.24−4.12 (m, 1H), 3.94 (qd, J = 9.5, 5.5, 2H), 3.60 (q, J = 8.1, 1H), 3.36 (td, J = 8.2, 4.4, 1H), 2.44 (s, 1H), 2.35−2.09 (m, 5H). ^{13}C NMR (100 MHz, $CDCl_3$): δ 154.4, 144.5, 138.0, 137.6, 132.2, 129.6, 128.7, 128.29, 122.9, 122.2, 120.5, 92.6, 85.5, 72.7, 57.0, 44.2, 23.8, 21.2. HRMS (ESI): exact mass calcd for $C_{18}H_{18}N_2O$ [M + H]$^+$, 279.1497; found, 279.1512. $[\alpha]_D^{25.5}$ = −8.4 (c = 1.9, $CHCl_3$). Anal. Calcd for $C_{18}H_{18}N_2O{\cdot}0.06CH_2Cl_2$: C, 76.19; H, 6.60; N, 9.87. Found: C, 75.84; H, 6.34, N, 9.75.

*(S)-3-(Azetidin-2-ylmethoxy)-5-((3-chlorophenyl)ethynyl)pyridine (**8**).* Route 2 (method i) in Scheme 1 was used and generated a yield of 72% (liquid). ^{1}H NMR (400 MHz, $CDCl_3$): δ 8.27 (d, J = 1.6, 1H), 8.20 (d, J = 2.8, 1H), 7.44 (t, J = 1.7, 1H), 7.33 (dt, J = 7.4, 1.4, 1H), 7.27−7.17 (m, 3H), 4.26−4.14 (m, 1H), 4.04−3.89 (m, 2H), 3.62 (q, J = 8.1, 1H), 3.43−3.32 (m, 1H), 2.38−2.11 (m, 3H). ^{13}C NMR (100 MHz, $CDCl_3$): δ 154.4, 144.5, 138.0, 134.2, 131.4, 129.7, 129.6, 128.9, 124.1, 122.9, 119.9, 90.7, 86.9, 72.8, 56.9, 44.2, 23.8. HRMS (ESI): exact mass calcd for $C_{17}H_{15}ClN_2O$ [M + H]$^+$, 299.0951; found, 299.0965. $[\alpha]_D^{25.6}$ = −8.1 (c = 1.6, $CHCl_3$). Anal. Calcd for $C_{17}H_{15}ClN_2O{\cdot}0.06H_2O$: C, 67.84; H, 5.04; N, 9.30. Found: C, 67.70, H, 5.03; N, 9.11.

*(S)-3-((5-(Azetidin-2-ylmethoxy)pyridin-3-yl)ethynyl)-5-fluoro-N,N-dimethylaniline (**9**).* Route 2 (method i) in Scheme 1 was used and generated a yield of 72% (liquid). ^{1}H NMR (400 MHz, $CDCl_3$): δ 8.29 (d, J = 1.6, 1H), 8.21 (t, J = 4.5, 1H), 7.26 (dd, J = 2.8, 1.7, 1H), 6.58−6.46 (m, 2H), 6.32 (dt, J = 12.5, 2.3, 1H), 4.21 (d, J = 15.8, 1H), 3.99 (qd, J = 9.5, 5.5, 2H),3.65 (q, J = 7.9, 1H), 3.41 (dd, J = 12.0, 8.3, 1H), 2.93−2.85 (s, 6H), 2.40−2.13 (m, 2H), 2.00 (d, J = 19.3, 1H). ^{13}C NMR (100 MHz, $CDCl_3$): δ 163.5 (d, J_{F-C} = 241 Hz), 154.4, 151.6 (d, J_{F-C} = 11 Hz), 144.6, 137.8, 123.8 (d, J_{F-C} =12 Hz), 123.0, 120.3, 111.1 (d, J_{F-C} = 2.0, 1H), 105.9 (d, J_{F-C} =24 Hz), 100.1 (d, J_{F-C} = 26 Hz), 92.3 (d, J_{F-C} = 4 Hz), 85.2, 72.7,57.0, 44.2, 40.3, 23.9. HRMS (ESI): exact mass calcd for $C_{19}H_{20}FN_3O$ [M + H]$^+$, 326.1669; found, 326.1668. $[\alpha]_D^{25.5}$ = −18.5 (c = 0.18, $CHCl_3$).

*(S)-3-(Azetidin-2-ylmethoxy)-5-((3-fluoro-5-methylphenyl)-ethynyl)pyridine (**10**).* Route 2 (method i) in Scheme 1 was used and generated a yield of 73% (liquid). ^{1}H NMR (400 MHz, $CDCl_3$): δ 8.33 (d, J = 1.6, 1H), 8.29−8.24 (m, 1H), 7.29 (dd, J = 2.8, 1.7, 1H), 7.12 (dt, J = 2.1, 0.7, 1H), 7.05−6.98 (m, 1H), 6.87 (dddd, J = 9.6, 2.3, 1.4, 0.7, 1H), 4.28 (tt, J = 12.3, 6.2, 1H), 4.03 (qd, J = 9.5, 5.5, 2H), 3.70 (dd, J = 15.9, 8.2, 1H), 3.45 (ddd, J = 7.6, 7.1, 4.4, 1H), 2.43−2.34 (m, 2H), 2.33 (t, J = 1.5, 3H), 2.25 (ddd, J = 16.4, 11.1, 8.2, 1H). ^{13}C NMR (100 MHz, $CDCl_3$): δ 162.3 (d, J_{F-C} = 246.3), 154.4, 144.6, 140.5 (d, J_{F-C} = 8.6), 138.0, 128.2 (d, J_{F-C} = 2.7), 123.7 (d, J_{F-C} = 10.3), 122.9, 120.1, 116.8 (d, J_{F-C} = 21.1), 115.4 (d, J_{F-C} = 23.1), 91.2 (d, J_{F-C} = 3.7), 86.2, 72.7, 57.0, 44.2, 23.8, 21.1. HRMS (ESI): exact mass calcd for $C_{18}H_{17}FN_2O$ [M + H]$^+$, 297.1403; found, 297.1403. $[\alpha]_D^{25.0}$ = −7.2 (c = 1.8, $CHCl_3$). Anal. Calcd for $C_{18}H_{17}FN_2O{\cdot}0.04H_2O$: C, 72.59; H, 5.76; N, 9.40. Found: C, 70.86; H, 5.72; N, 9.01.

*(S)-3-(Azetidin-2-ylmethoxy)-5-((3-fluoro-5-methoxyphenyl)-ethynyl)pyridine (**11**).* Route 2 (method i) in Scheme 1 was used and generated a yield of 66% (liquid). ^{1}H NMR (400 MHz, $CDCl_3$): δ 8.29 (d, J = 1.6, 1H), 8.22 (d, J = 2.8, 1H), 7.25 (dd, J = 2.8, 1.7, 1H), 6.83−6.72 (m, 2H), 6.57 (dt, J = 10.6, 2.3, 1H), 4.22 (s, 1H), 4.06−3.92 (m, 2H), 3.75 (s, 3H), 3.64 (s, 1H), 3.39 (s, 1H), 2.54−1.91 (m, 3H).^{13}C NMR (100 MHz, $CDCl_3$): δ 163.1 (d, J_{F-C} = 245.6), 160.7 (d, J_{F-C} = 12.1), 154.4, 144.6, 138.1, 124.3 (d, J_{F-C} = 12.1), 123.0, 119.9, 112.8 (d, J_{F-C} = 2.9), 110.9 (d, J_{F-C} = 23.6), 103.2 (d, J_{F-C} = 25.0), 91.1 (d, J_{F-C} = 4.2), 86.4, 72.8, 57.0, 55.6, 44.2, 23.9. HRMS (ESI): exact mass calcd for $C_{18}H_{17}FN_2O_2$ [M + H]$^+$, 313.1352; found, 313.1358. $[\alpha]_D^{25.2}$ = −8.3 (c = 0.4, $CHCl_3$). Anal. Calcd for $C_{18}H_{17}FN_2O_2{\cdot}0.04H_2O$: C, 68.89; H, 5.47; N, 8.92. Found: C, 67.51; H, 5.51; N, 8.60.

*3-(Cyclobutylmethoxy)-5-(phenylethynyl)pyridine (**12**).* Methods of b, c, d in Scheme 2A was used and generated a yield of 65% (liquid). ^{1}H NMR (400 MHz, $CDCl_3$): δ 8.36 (d, J = 1.5, 1H), 8.26 (d, J = 2.8, 1H), 7.60−7.50 (m, 2H), 7.40−7.33 (m, 3H), 7.34−7.28 (m, 1H), 3.98 (d, J = 6.6, 2H), 2.88−2.73 (m, 1H), 2.23−2.10 (m, 2H), 2.07−1.82 (m, 4H). ^{13}C NMR (100 MHz, $CDCl_3$): δ 154.7, 144.3, 137.8, 131.6, 128.7, 128.4, 122.8, 122.5, 120.4, 92.2, 85.9, 72.4, 34.4, 24.7, 18.5. HRMS (ESI): exact mass calcd for $C_{18}H_{17}NO$ [M + H]$^+$, 264.1388, found 264.1396. Anal. Calcd for $C_{18}H_{17}NO$: C, 82.10; H, 6.51; N, 5.32. Found: C, 81.94; H, 6.44; N, 5.31.

*N-(2-(5-(Phenylethynyl)pyridin-3-yloxy)ethyl)propan-1-amine (**13**).* Method e in Scheme 2B was used and generated a yield of 87% (solid). ^{1}H NMR (400 MHz, $CDCl_3$): δ 8.29 (d, J = 1.5, 1H), 8.19 (d, J = 2.8, 1H), 7.50−7.41 (m, 2H), 7.33−7.26 (m, 3H), 7.26−7.22 (m, 1H),4.05 (t, J = 5.2, 2H), 2.96 (t, J = 5.2, 2H), 2.58 (t, J = 7.2, 2H), 1.47 (td, J = 14.6, 7.3, 3H), 0.87 (t, J = 7.4, 3H).^{13}C NMR (100 MHz, $CDCl_3$): δ 154.3, 144.6, 137.7, 131.6, 128.7, 128.4, 122.8, 122.4, 120.5, 92.3, 85.8, 68.0, 51.7, 48.5, 23.1, 11.7. HRMS (ESI): exact mass calcd for $C_{18}H_{20}N_2O$ [M + H]$^+$, 281.1654; found, 281.1645. Anal. Calcd for $C_{18}H_{20}N_2O$: C, 77.11; H, 7.19; N, 9.99. Found: C, 76.81; H, 7.12; N, 9.84.

*(R)-3-(Azetidin-2-ylmethoxy)-5-(phenylethynyl)pyridine (**14**).* Method e in Scheme 2C was used and generated a yield of 75% (liquid). ^{1}H NMR (400 MHz, $CDCl_3$): δ 8.28 (s, 1H), 8.19 (d, J = 2.8, 1H), 7.51−7.42 (m, 2H), 7.27 (ddd, J = 10.0, 6.0, 0.8, 4H), 4.26−4.14 (m, 1H), 3.96 (qd, J = 9.5, 5.7, 2H), 3.62 (q, J = 8.0, 1H), 3.38 (td, J = 8.1, 4.4, 1H), 2.38−2.12 (m, 3H). ^{13}C NMR (100 MHz, $CDCl_3$): δ 154.4, 144.6, 137.7, 131.6, 128.7, 128.4, 122.9, 122.4, 120.5, 92.3, 85.8, 72.7, 57.0, 44.2, 23.9. HRMS (ESI): exact mass calcd for $C_{17}H_{16}N_2O$ [M + H]$^+$, 265.1341; found, 265.1349. $[\alpha]_D^{24.1}$ = +13.6 (c = 0.7, $CHCl_3$). Anal. Calcd for $C_{17}H_{16}N_2O{\cdot}0.6H_2O$: C, 74.21; H, 6.30; N, 10.18. Found: C, 74.50; H, 6.20; N, 10.07.

*(S)-3-((1-Methylazetidin-2-yl)methoxy)-5-(phenylethynyl)pyridine (**15**).* Method f in Scheme 2D was used and generated a yield of 48% (liquid). (S)-3-(Azetidin-2-ylmethoxy)-5-(phenylethynyl) pyridine (compound **1**, 0.12 mmol) was taken in a 2 mL of ethanol. Formalin (37%, 0.3 mL) was added, and the acidity was adjusted to pH 5 with the addition of acetic acid and sodium acetate. The reaction mixture was stirred for 15 min. Sodium cyanoborohydride (0.38 mmol) was added. The whole reaction mixture was allowed to stir for 18 h at room temperature. The solvent was evaporated, and the crude product was purified by column chromatography to yield pure **15**. ^{1}H NMR (400 MHz, $CDCl_3$): δ 8.30 (d, J = 1.4, 1H), 8.20 (d, J = 2.8, 1H), 7.52−7.43 (m, 2H), 7.32−7.28 (m, 3H), 7.25 (dd, J = 2.7, 1.7, 1H), 4.06−3.95 (m, 2H), 3.51−3.35 (m, 2H), 2.86 (dd, J = 15.9, 8.6, 1H), 2.37 (s, 3H), 2.05 (td, J = 8.7, 6.0, 2H). ^{13}C NMR (100 MHz, $CDCl_3$): δ 154.3, 144.6, 137.7, 131.6, 128.7, 128.4, 123.0, 122.4, 120.5, 92.3, 85.8, 71.5, 66.0, 53.4, 44.8, 20.3. HRMS (ESI): exact mass calcd for $C_{18}H_{18}N_2O$ [M + H]$^+$, 279.149; found, 279.1513. $[\alpha]_D^{24.5}$ = −32.2 (c = 0.3, $CHCl_3$).

*(S)-3-(Azetidin-2-ylmethoxy)-5-phenylpyridine (**16**).* Methods of a and b in Scheme 3 was used and generated a yield of 71% (liquid). To a solution of (S)-*tert*-butyl 2-((5-bromopyridin-3-yloxy)methyl)-azetidine-1-carboxylate (**18**, 0.58 mmol) in 9 mL of toluene and 3 mL of ethanol was added phenyl boronic acid (**41**, 0.69 mmol) followed by 2 mL of 2 M Na_2CO_3 and tetrakis(triphenylphosphine)-palladium (0) (0.03 mmol). The reaction was stirred for 12 h at 90 °C under nitrogen. The reaction was cooled to room temperature, diluted with water, and extracted three times with ethyl acetate. The combined organic layers dried over anhydrous sodium sulfate, filtered, and concentrated in vacuo to afford a crude product, which was subsequently purified by column chromatography. The resulting pure compound was subjected to Boc deprotection followed by purification of column chromatography to yield a final pure compound **16**. ^{1}H NMR (400 MHz, $CDCl_3$): δ 8.37 (d, J = 1.7, 1H), 8.22 (d, J =

2.7, 1H), 7.49 (dd, J = 5.1, 3.8, 2H), 7.38 (t, J = 7.6, 2H), 7.31 (ddd, J = 7.7, 4.1, 0.5, 2H), 4.31−4.14 (m, 1H), 4.02 (qd, J = 9.5, 5.6, 2H), 3.63 (q, J = 8.0, 1H), 3.39 (td, J = 8.2, 4.4, 1H), 2.39−2.13 (m, 3H). ^{13}C NMR (100 MHz, $CDCl_3$): δ 155.1, 140.7, 137.6, 137.2, 136.5, 128.9, 128.1, 127.1, 119.7, 72.8, 57.1, 44.2, 24.0. HRMS (ESI): exact mass calcd for $C_{15}H_{16}N_2O$ [M + H]$^+$, 241.1341; found, 241.1348. $[\alpha]_D^{25.5}$ = −4.69(c = 1.4, $CHCl_3$). Anal. Calcd for $C_{15}H_{16}N_2O{\cdot}0.6H_2O$: C, 71.74; H, 6.90; N, 11.15. Found: C, 71.73; H, 6.76; N, 10.88.

*(S)-tert-Butyl-2-((5-bromopyridin-3-yloxy)methyl)azetidine-1-carboxylate (**18**).* Mitsunobu reaction conditions were applied and generated a yield of 55% (white solid). ^{1}H NMR (400 MHz, $CDCl_3$): δ 8.25−8.19 (m, 2H), 7.36 (s, 1H), 4.44 (d, J = 5.3, 1H), 4.32−4.20 (m, 1H), 4.06 (dd, J = 2.8, 10.1, 1H), 3.81 (t, J = 7.5, 2H), 2.36−2.14 (m, 2H), 1.36 (s, 9H). ^{13}C NMR (100 MHz, $CDCl_3$): δ 156.1,155.4,143.1, 136.7, 124.0, 120.3, 79.8, 69.0, 59.9, 47.1, 28.3, 18.95. HRMS (ESI): exact mass calcd for $C_{14}H_{19}BrN_2O_3$ [M + H]$^+$, 343.0657; found, 343.0670.

*(S)-tert-Butyl-2-((5-((trimethylsilyl)ethynyl)pyridin-3-yloxy)-methyl)azetidine-1-carboxylate (**20**).* Sonogashira coupling method (route 1 (method b) in Scheme1) was applied and generated a yield of 62% (liquid). ^{1}H NMR (400 MHz, $CDCl_3$): δ 8.04 (s, 2H), 7.08 (d, 1H), 4.26 (s, 1H), 4.09 (s, 1H), 3.89 (s,1H), 3.63 (s, 2H), 2.07 (d, 2H), 1.18 (s, 9H), 0.16 (s, 9H). ^{13}C NMR (100 MHz, $CDCl_3$): δ 156.2, 154.5, 145.2, 138.4, 123.4, 120.5, 101.5, 98.1, 79.7, 68.9, 60.2, 47.3, 28.6, 19.2, 0.3.

*(S)-tert-Butyl-2-((5-ethynylpyridin-3-yloxy)methyl)azetidine-1-carboxylate (**21**).* Route 1 (method c) in Scheme 1 was applied. ^{1}HNMR (400 MHz, $CDCl_3$): δ 8.36 (s, 2H), 7.35 (s, 1H), 4.65−4.46 (m, 1H), 4.35 (s, 1H), 4.16 (dd, J = 2.9, 10.1, 1H), 3.91 (t, J = 7.6, 2H), 3.22 (s, 1H), 2.50−2.19 (m, 2H), 1.45 (s, 9H). ^{13}C NMR (100 MHz, $CDCl_3$): δ 156.1, 155.5, 145.2, 138.5, 123.7, 80.4, 80.1, 79.8, 68.8, 60.0, 47.1, 28.4, 19.0.

*(S)-tert-Butyl-2-((5-(phenylethynyl)pyridin-3-yloxy)methyl)-azetidine-1-carboxylate (**22**).* Both routes 1 and 2 in Scheme 1 were used and generated a yield of 54% (liquid). ^{1}H NMR (400 MHz, $CDCl_3$): δ 8.39 (s, 1H), 8.31 (s, 1H), 7.59−7.51 (m, 2H), 7.37 (ddd, J = 1.5, 3.4, 5.9, 4H), 4.62−4.44 (m, 1H), 4.36 (s, 1H), 4.16 (dd, J = 2.9, 10.1, 1H), 3.90 (t, J = 7.6, 2H), 2.51−2.19 (m, 2H), 1.44 (s, 9H). ^{13}C NMR (100 MHz, $CDCl_3$): δ 156.1, 154.5, 144.8, 137.9, 131.6, 128.8, 128.4, 122.9, 122.4, 120.6, 92.4, 85.8, 79.7, 68.8, 60.0, 47.0, 28.4, 19.0. HRMS (ESI): exact mass calcd for $C_{22}H_{24}N_2O_3$ [M + H]$^+$, 365.1870; found, 365.1870.

*(S)-tert-Butyl-2-((5-((4-fluorophenyl)ethynyl)pyridin-3-yloxy)-methyl)azetidine-1-carboxylate (**23**).* Route 1 (method d) in Scheme 1 was used and generated a yield of 63% (liquid). ^{1}H NMR (400 MHz, $CDCl_3$): δ 8.37 (d, J = 1.0, 1H), 8.31 (d, J = 2.8, 1H), 7.57−7.50 (m, 2H), 7.40−7.35 (m, 1H),7.12−7.03 (m, 2H), 4.58−4.50 (m, 1H), 4.36 (s, 1H), 4.16 (dd, J = 2.9, 10.1, 1H), 3.90 (t, J = 7.6, 2H), 2.53−2.18 (m, 2H), 1.44 (s, 9H). ^{13}C NMR (100 MHz, $CDCl_3$): δ 162.7(d, J_{F-C} = 250 Hz), 156.0, 154.5, 144.6, 137.9, 133.6 (d, J_{F-C} = 8.4 Hz,), 122.9, 120.4, 118.5 (d, J_{F-C} = 3.6), 115.7(d, J_{F-C} = 22), 91.3, 85.5 (d, J_{F-C} = 1.3) 79.7, 68.7, 60.0, 47.1, 28.3, 19.0. HRMS (ESI): exact mass calcd for $C_{22}H_{23}FN_2O3$ [M + H]$^+$, 383.1771; found, 383.1767.

*(S)-tert-Butyl-2-((5-((2-fluorophenyl)ethynyl)pyridin-3-yloxy)-methyl)azetidine-1-carboxylate (**24**).* Route 1 (method d) in Scheme 1 was used and generated a yield of 77% (liquid). ^{1}H NMR (400 MHz, $CDCl_3$): δ 8.32 (d, J = 4.1, 1H), 8.24 (dd, J = 2.8, 5.7, 1H), 7.45 (d, J = 5.4, 1H), 7.29 (d, J = 16.2, 2H), 7.06 (dd, J = 9.0, 10.1, 2H), 4.45 (s, 1H), 4.28 (s, 1H), 4.08 (dd, J = 3.4, 6.6, 1H), 3.88−3.72 (m, 2H), 2.25 (m, 2H), 1.35 (s, 9H). ^{13}C NMR (100 MHz, $CDCl_3$): δ 162.61 (d, J_{F-C} =251 Hz), 156.0, 154.4, 144.7, 138.2, 133.4 (d, J_{F-C} = 0.9), 130.5 (d, J_{F-C} = 8.0), 124.0 (d, J_{F-C} = 3.8), 122.9,120.1, 115.5 (d, J_{F-C} =21 Hz), 111.1(d, J_{F-C} =15 Hz), 90.7 (d, J_{F-C} = 3.2 Hz), 85.7, 79.7, 68.7, 60.0, 28.3, 47.1, 19.0. HRMS (ESI): exact mass calcd for $C_{22}H_{23}FN_2O_3$ [M + H]$^+$, 383.1771; found. 383.1784.

*(S)-tert-Butyl-2-((5-((3-fluorophenyl)ethynyl)pyridin-3-yloxy)-methyl)azetidine-1-carboxylate (**25**).* Route 1 (method d) in Scheme 1 was used and generated a yield of 48% (liquid). ^{1}H NMR (400 MHz, $CDCl_3$): δ 8.30 (s, 1H), 8.24 (d, J = 2.6, 1H), 7.26 (ddd, J = 12.6, 8.1, 1.1, 3H), 7.20−7.12 (m, 1H), 7.05−6.94 (m, 1H), 4.45 (s, 1H), 4.29 (s, 1H), 4.08 (dd, J = 10.1, 2.8, 1H), 3.82 (t, J = 7.5, 2H), 2.41−2.12 (m, 2H), 1.37 (s, 9H). ^{13}C NMR (100 MHz, $CDCl_3$): δ 162.3 (d, J_{F-C} = 246 Hz), 156.1, 154.5, 144.7, 138.2, 130.0 (d, J_{F-C} = 8.6, 7H), 127.5 (d, J_{F-C} = 3.1), 124.3 (d, J_{F-C} = 9 Hz), 123.0, 120.1, 118.4 (d, J_{F-C} = 23 Hz), 116.1 (d, J_{F-C} =21 Hz), 91.0 (d, J_{F-C} = 3.4), 86.6, 79.7, 68.8, 60.0, 47.1, 28.4, 19.0. HRMS (ESI): exact mass calcd for $C_{22}H_{23}FN_2O_3$ [M + H]$^+$, 383.1771; found, 383.1778.

*(S)-tert-Butyl-2-((5-((3,5-difluorophenyl)ethynyl)pyridin-3 yloxy)-methyl)azetidine-1-carboxylate (**26**).* Route 2 (methods of f, g, h) in Scheme 1 was used and generated a yield of 60% (liquid). ^{1}H NMR (400 MHz, $CDCl_3$): δ 8.30 (s, 1H), 8.26 (d, J = 2.8, 1H), 7.30 (s, 1H), 7.02−6.93 (m, 2H), 6.76 (tt, J = 8.9, 2.2, 1H), 4.54−4.40 (m, 1H), 4.29 (s, 1H), 4.15−4.03 (m, 1H), 3.82 (t, J = 7.6, 2H), 2.40−2.12 (m, 2H), 1.36 (s, 9H). ^{13}C NMR (100 MHz, $CDCl_3$): δ 163.9 (d, J_{F-C} = 13 Hz), 161.4 (d, J_{F-C} = 13 Hz), 156.1, 154.4, 144.7, 138.5, 125.1(t), 123.0, 119.5, 114.6 (d, J_{F-C} = 7.7), 114.4 (d, J_{F-C} = 7.6), 104.9 (t), 89.8, 87.6, 79.7, 68.8, 60.0, 47.1, 28.3, 18.9. HRMS (ESI): exact mass calcd for $C_{22}H_{22}F_2N_2O_3$ [M + H]$^+$, 401.1677; found, 401.1692.

*(S)-tert-Butyl-2-((5-((3-(trifluoromethyl)phenyl)ethynyl)pyridin-3yloxy)methyl)azetidine-1-carboxylate (**27**).* Route 2 (methods of f, g, h) in Scheme 1 was used and generated a yield of 50% (liquid). ^{1}H NMR (400 MHz, $CDCl_3$): δ 8.39 (d, J = 1.4, 1H), 8.33 (d, J = 2.8, 1H), 7.80 (s, 1H), 7.70 (d, J = 7.8, 1H), 7.61 (d, J = 7.9, 1H), 7.50 (t, J = 7.8, 1H), 7.40 (d, J = 1.8, 1H), 4.53 (dd, J = 5.4, 8.1, 1H), 4.37 (s, 1H), 4.22−4.10 (m, 1H), 3.90 (t, J = 7.6, 2H), 2.49−2.17 (m, 2H), 1.55−1.32 (m, 9H). ^{13}C NMR (100 MHz, $CDCl_3$): δ 156.0, 154.4, 144.6, 138.4, 134.6, 130.9, 128.9, 128.3, 125.1, 123.4, 122.9, 119.7, 90.6, 87.2, 79.6, 68.7, 60.0,47.1, 28.3, 18.9. HRMS (ESI): exact mass calcd for $C_{23}H_{23}F_3N_2O_3$ [M + H]$^+$, 433.1739; found, 433.1749.

*(S)-tert-Butyl-2-((5-(m-tolylethynyl)pyridin-3-yloxy)methyl)-azetidine-1-carboxylate (**28**).* Route 2 (methods of f, g, h) in Scheme 1 was used and generated a yield of 56% (liquid). ^{1}H NMR (400 MHz, $CDCl_3$): δ 8.38 (d, J = 1.6, 1H), 8.30 (d, J = 2.8, 1H), 7.40−7.33 (m, 3H), 7.29−7.24 (m, 1H), 7.19 (d, J = 7.6, 1H), 4.59−4.48 (m, 1H), 4.36 (s, 1H), 4.22−4.12 (m, 1H), 3.90 (t, J = 7.6, 2H), 2.43−2.33 (s, 3H), 1.44 (s, 9H). ^{13}C NMR (100 MHz, $CDCl_3$): δ 156.0, 154.4, 144.7, 138.0, 137.8, 132.2, 129.6, 128.7, 128.3, 122.9, 122.2, 120.6, 92.6, 85.4, 79.7, 68.7, 60.0, 47.0, 28.4, 21.1, 19.0. HRMS (ESI): exact mass calcd for $C_{23}H_{26}N_2O_3$ [M + H]$^+$, 379.2022; found, 379.2031.

*(S)-tert-Butyl-2-((5-((3-chlorophenyl)ethynyl)pyridin-3yloxy)-methyl)azetidine-1-carboxylate(**29**).* Route 2 (methods of f, g, h) in Scheme1 was used and generated a yield of 65% (liquid). ^{1}H NMR (400 MHz, $CDCl_3$): δ 8.29 (d, J = 1.5, 1H), 8.24 (d, J = 2.8, 1H), 7.44 (dd, J = 2.5, 0.9, 1H), 7.33 (dt, J = 7.4, 1.5, 1H), 7.28 (ddd, J = 3.4, 2.4, 1.5, 1H), 7.25 (dd, J = 2.0, 1.4, 1H),7.24−7.18 (m, 1H), 4.56−4.38 (m, 1H), 4.28 (s, 1H), 4.08 (dd, J = 10.1, 2.9, 1H), 3.81 (t, J = 7.6, 2H), 2.37−2.12 (m, 2H), 1.35 (s, 9H). ^{13}C NMR (100 MHz, $CDCl_3$): δ 156.0, 154.4, 144.7, 138.2, 134.2, 131.4, 129.7, 129.6, 128.9, 124.1,122.9, 120.0, 90.8, 86.9, 79.7, 68.7, 60.0, 47.0, 28.3, 19.02. HRMS (ESI): exact mass calcd for $C_{22}H_{23}ClN_2O_3$ [M + H]$^+$, 399.1475; found, 399.1456.

*(S)-tert-Butyl-2-((5-((3-(dimethylamino)-5-fluorophenyl)ethynyl)-pyridin-3-yloxy)methyl)azetidine-1-carboxylate (**30**).* Route 2 (methods of f, g, h) in Scheme 1 was used and generated a yield of 14% (liquid). ^{1}H NMR (400 MHz, $CDCl_3$): δ 8.35 (s, 1H), 8.27 (s, 1H), 7.35 (s, 1H), 6.60 (s, 1H), 6.54 (d, J = 8.7, 1H), 6.37 (dt, J = 12.4, 2.2, 1H), 4.49 (s, 1H), 4.33 (s, 1H), 4.19−4.08 (m, 1H), 3.87 (t, J = 7.6, 2H), 2.94 (d, J = 9.7, 6H), 2.43−2.20 (m, 2H), 1.40 (s, 9H). ^{13}C NMR (100 MHz, $CDCl_3$): δ 163.5 (d, J_{F-C} = 241 Hz), 156.1, 154.4, 151.6 (d, J_{F-C} = 12 Hz), 144.8, 138.0, 123.8 (d, J_{F-C} = 12 Hz), 123.0, 111.13 (d, J_{F-C} = 2.0), 106.45 (d, J_{F-C} = 76 Hz), 100.1 (d, J_{F-C} = 26 Hz), 92.42 (d, J_{F-C} = 4.2), 85.1, 79.7, 68.8 (d, J_{F-C} = 3 Hz), 60.0, 47.0, 40.2, 28.4, 19.0.

*(S)-tert-Butyl-2-((5-((3-fluoro-5-methylphenyl)ethynyl)pyridin-3-yloxy)methyl)azetidine-1-carboxylate (**31**).* Route 2 (methods of f, g, h) in Scheme 1 was used and generated a yield of 65% (liquid). ^{1}H NMR (400 MHz, $CDCl_3$): δ 8.28 (d, J = 1.5, 1H), 8.22 (d, J = 2.8, 1H), 7.28 (dd, J = 2.6, 1.7, 1H), 7.06 (d, J = 0.5, 1H), 6.94 (dd, J = 9.1, 0.5, 1H), 6.80 (d, J = 9.5, 1H), 4.51−4.39 (m, 1H), 4.27 (s, 1H), 4.12−4.00 (m, 1H), 3.81 (t, J = 7.6, 2H), 2.35−2.09 (m, 5H), 1.35 (s,

9H). ^{13}C NMR (100 MHz, $CDCl_3$): δ 162.3 (d, J_{F-C} = 245 Hz), 156.1, 151.4, 144.7, 140.5 (d, J_{F-C} = 8 Hz), 138.1, 128.2 (d, J_{F-C} = 2.8, 3H), 123.7 (d, J_{F-C} = 11 Hz), 123.0, 120.1, 116.8 (d, J_{F-C} = Hz), 115.4 (d, J_{F-C} = 23 Hz), 91.3 (d, J_{F-C} 3.7), 86.1, 79.7, 68.8, 60.0, 47.2, 28.3, 21.1, 19.0. HRMS (ESI): exact mass calcd for $C_{23}H_{25}FN_2O_3$ [M + H]$^+$, 397.1927; found, 397.1929.

*(S)-tert-Butyl-2-((5-((3-fluoro-5-methoxyphenyl)ethynyl)pyridin-3-yloxy)methyl)azetidine-1-carboxylate (**32**).* Route 2 (methods f, g, h) in Scheme 1 was used and generated a yield of 37% (liquid). ^{1}H NMR (400 MHz, $CDCl_3$): δ 8.27 (s, 1H), 8.21 (d, J = 2.7, 1H), 7.31−7.24 (m, 1H), 6.74 (ddd, J = 1.2, 2.1, 9.9, 2H), 6.54 (dt, J = 2.3, 10.6, 1H), 4.47−4.38 (m, 1H), 4.25 (s, 1H), 4.09−4.02 (m, 1H), 3.79 (t, J = 7.6, 2H), 3.72 (s, 3H), 2.32−2.13 (m, 2H), 1.32 (s, 9H). ^{13}C NMR (100 MHz, $CDCl_3$): δ 163.1 (d, J_{F-C} = 245.8), 160.7 (d, J_{F-C} = 12.1), 156.1, 154.5, 144.8, 138.2, 124.34 (d, J_{F-C} = 12.1), 123.0, 120.0, 112.8 (d, J_{F-C} = 2.9), 110.9 (d, J_{F-C} = 23.5), 103.2 (d, J_{F-C} = 25.0), 91.2, 86.3, 79.7, 68.8, 60.0, 55.6, 47.3, 28.4, 19.05. HRMS (ESI): exact mass calcd for $C_{23}H_{25}FN_2O_4$ [M + H]$^+$, 413.1877; found, 413.1887.

*3-Bromo-5-(cyclobutylmethoxy)pyridine (**34**).* Method a in Scheme 2A was used and generated a yield of 69% (liquid). ^{1}H NMR (400 MHz, $CDCl_3$): δ 8.18 (dd, J = 11.0, 2.1, 2H), 7.28 (dd, J = 2.5, 1.9, 1H), 3.88 (dd, J = 6.4, 3.4, 2H), 2.78−2.64 (m, 1H), 2.14−2.02 (m, 2H), 1.99−1.74 (m, 4H). ^{13}C NMR (100 MHz, $CDCl_3$): δ 155.4, 142.3, 136.3, 123.4, 120.1, 72.3, 34.1, 24.5, 18.40. HRMS (ESI): exact mass calcd for $C_{10}H_{12}BrNO$ [M + H]$^+$, 242.0181; found, 242.0181.

*tert-Butyl-2-(5-bromopyridin-3-yloxy)ethyl(propyl)carbamate (**36**).* Method a in Scheme 2B was used and generated a yield of 62% (liquid). ^{1}H NMR 400 MHz, $CDCl_3$): δ 8.21 (s, 1H), 8.15 (d, J = 2.5, 1H), 7.29 (s, 1H), 4.06 (s, 2H), 3.51 (s, 2H), 3.16 (s, 2H), 1.56−1.43 (m, 2H), 1.39 (s, 9H), 0.82 (t, J = 7.4, 3H). ^{13}C NMR (100 MHz, $CDCl_3$): δ 155.0, 142.7, 136.3, 123.4, 120.1, 79.3, 67.0, 50.4, 46.6, 28.2, 21.8, 11.0. HRMS (ESI): exact mass calcd for $C_{15}H_{23}BrN_2O_3$ [M + H]$^+$, 359.0970; found, 359.0978.

*tert-Butyl-2-(5-(phenylethynyl)pyridin-3-yloxy)ethyl(propyl)-carbamate (**37**).* Methods of b, c, d in Scheme 2B was used and generated a yield of 53% (solid). ^{1}H NMR (400 MHz, $CDCl_3$): δ 8.37 (s, 1H), 8.25 (d, J = 2.8, 1H), 7.59−7.49 (m, 2H), 7.37−7.28 (m, 4H), 4.14 (s, 2H), 3.59 (s, 2H), 3.25 (s, 2H), 1.64−1.51 (m, 2H), 1.47 (s, 9H), 0.89 (t, J = 7.4, 3H). ^{13}C NMR (100 MHz, $CDCl_3$): δ 155.6, 154.2, 144.5, 137.6, 131.6, 128.7, 128.3, 122.6, 122.4, 120.5, 92.4, 85.8, 79.5, 66.9, 50.5, 46.8, 28.3, 21.9, 11.1. HRMS (ESI): exact mass calcd for $C_{23}H_{28}N_2O_3$ [M + H]$^+$, 381.2187; found, 381.2169

*(R)-tert-Butyl-2-((5-bromopyridin-3-yloxy)methyl)azetidine-1-carboxylate (**39**).* Method a in Scheme 2C was used and generated a yield of 30% (solid). ^{1}H NMR (400 MHz, $CDCl_3$): δ 8.20 (d, J = 2.4, 2H), 7.35 (t, J = 1.9, 1H), 4.48−4.40 (m, 1H), 4.26 (s, 1H), 4.05 (dd, J = 10.1, 2.7, 1H), 3.86−3.76 (m, 2H), 2.70−2.01 (m, 2H), 1.35 (s, 9H). ^{13}C NMR (100 MHz, $CDCl_3$): δ 156.0, 155.4, 143.1, 136.6, 124.0, 120.3, 79.7, 69.0, 59.9, 47.0, 28.3, 18.9. HRMS (ESI): exact mass calcd for $C_{14}H_{19}BrN_2O_3$ [M + H]$^+$, 343.0657; found, 343.0680.

*(R)-tert-Butyl-2-((5-(phenylethynyl)pyridin-3-yloxy)methyl)-azetidine-1-carboxylate (**40**).* Methods of b, c, d in Scheme 2C were used and generated a yield of 74% (liquid). ^{1}H NMR (400 MHz, $CDCl_3$): δ 8.31 (s, 1H), 8.23 (s, 1H), 7.52−7.41 (m, 2H), 7.36−7.24 (m, 4H), 4.45 (d, J = 5.4, 1H), 4.28 (s, 1H), 4.08 (dd, J = 10.2, 2.6, 1H), 3.82 (t, J = 7.6, 2H), 2.28 (ddd, J = 25.0, 14.3, 7.1, 2H), 1.36 (d, J = 0.5, 9H). ^{13}C NMR (100 MHz, $CDCl_3$): δ 156.1, 154.5, 144.7, 137.8, 131.6, 128.7, 128.4, 123.0, 122.4, 120.6, 92.4, 85.7, 79.7, 68.8, 47.0, 60.0, 28.4, 19.0. HRMS (ESI): exact mass calcd for $C_{22}H_{24}N_2O_3$ [M + H]$^+$, 365.1865; found, 343.1893.

Computational Studies. To study (S)-(−)-nicotine and (R)-(−)-deschloroepibatidine binding with the $\alpha4\beta2$ nAChR in atomic detail, a structural model of the LBD of human $\alpha4\beta2$ nAChR was built by using the Homology Model software MODELLERX9.10.[62] The reference template is the X-ray crystal structure of the AChBP (PDB entry of 1UW6) and the rat $\alpha4\beta2$ X-ray structure (PDB: 1OLE). Multiple sequence alignment was generated by Psi-BLAST[63] and ClusterW.[64] Upon construction of the model, appropriate ionization states were maintained, the side chains were relaxed to remove possible side chain atom contacts with the neighboring residues, different rotamer states of the residue were assigned, and then local side chain atom dynamics followed by minimization were performed. Minimization and molecular dynamics simulations were carried out using the SANDER module of AMBER 10.0[65] with default parameters. The homology modeled structure was validated with PROCHECK[66] and WHATIF program.[67]

Molecular docking was carried out using SurFlexDock Module of Sybyl-X (Tripos Inc. St. Louis, USA). However, to be consistent with the nicotine structural conformation (PDB: 1UW6), a manual intervention followed by constrained molecular dynamics simulations were carried out. This procedure was applied to compound **1**, varinicline, and sazetidine A. The $\alpha4\beta2$ nAChR compound complexes were refined by molecular dynamics simulation using the Amber 10.0[65] with the PARM98 force-field parameter. The charge and force field parameters of the compounds were obtained using the most recent Antechamber module in the Amber 10.0 (4), where compounds were minimized at the MP2/6-31G* level using Gaussian 09.[68] The SHAKE algorithm[69] was used to keep all bonds involving hydrogen atoms rigid. Weak coupling temperature and pressure coupling algorithms[70] were used to maintain constant temperature and pressure, respectively. Electrostatic interactions were calculated with the Ewald particle mesh method[71] with a dielectric constant at $1R_{ij}$ and a nonbonded cutoff of 12 Å for the real part of electrostatic interactions and for van der Waals interactions. The total charge of the system was neutralized by addition of a chloride ion. The system was solvated in a 12 Å cubic box of water where the TIP3P model was used. 5000 steps of minimization of the system were performed in which the $\alpha4\beta2$ nAChR was constrained by a force constant of 75 kcal/mol/Å. After minimization, a 20 ps simulation was used to gradually raise the temperature of the system to 298 K while the complex was constrained by a force constant of 20 kcal/mol/Å. Another 20 ps equilibration run was used where only the backbone atoms of the complex were constrained by a force constant of 5 kcal/mol/Å. Final production run of 200 ps was performed with no constraints. When applying constraints, the initial complex structure was used as a reference structure. The PME method was used and the time step was 5 fs, and a neighboring pairs list was updated every 25 steps.

General Procedure for in Vitro Studies. *Cell Lines and Cell Culture.* The cell line expressing rat $\alpha3\beta4$ nAChRs, KX$\alpha3\beta4$R2, was established previously by stably transfecting HEK 293 cells with combinations of rat nAChR $\alpha3$ and $\beta4$ subunit genes.[72,73] The cell line expressing human $\alpha4\beta2$ nAChRs, YX$\alpha4\beta2$H1, were established recently (Tuan et al., 2012, manuscript in preparation). These cell lines were maintained in minimum essential medium (MEM) supplemented with 10% fetal bovine serum, 100 units/mL penicillin G, 100 mg/mL streptomycin, and selective antibiotics at 37 °C with 5% CO_2 in a humidified incubator. Tissue culture medium and antibiotics were obtained from Invitrogen Corporation (Carlsbad, CA), unless otherwise stated. Fetal bovine serum and horse serum were provided by Gemini Bio-Products (Woodland, CA).

[^{3}H]Epibatidine Radioligand Binding Assay. Stably transfected cell lines, tissue culture conditions, membrane preparation procedures, and binding assays were described previously.[72−74] Briefly, cultured cells at >80% confluence were removed from their flasks (80 cm^2) with a disposable cell scraper and placed in 10 mL of 50 mM Tris·HCl buffer (pH 7.4, 4 °C). The cell suspension was centrifuged at 10000g for 5 min, and the pellet was collected. The cell pellet was then homogenized in 10 mL of buffer with a polytron homogenizer and centrifuged at 36000g for 10 min at 4 °C. The membrane pellet was resuspended in fresh buffer, and aliquots of the membrane preparation were used for binding assays. The concentration of [^{3}H]epibatidine used was ∼500 pM for competition binding assays. Nonspecific binding was assessed in parallel incubations in the presence of 300 μM nicotine. Bound and free ligands were separated by vacuum filtration through Whatman GF/C filters treated with 0.5% polyethylenimine. The filter-retained radioactivity was measured by liquid scintillation counting. Specific binding was defined as the difference between total binding and nonspecific binding. Data from competition binding

assays were analyzed using Prism 5 (GraphPad Software, San Diego, CA).

Binding Assays for Targets Other than nAChRS. All binding assays for targets other than nAChRs were performed by the National Institute of Mental Health's Psychoactive Drug Screening Program (PDSP) supported by NIMH grant HHSN-271-2008-00025-C (PI: Bryan Roth). For experimental details (K_i determinations, receptor binding profiles, functional data, MDR1 data, etc., as appropriate), refer to the PDSP Web site http://pdsp.med.unc.edu/.

$^{86}Rb^+$ Efflux Assay. Functional properties of compounds at nAChRs expressed in the transfected cells were measured using $^{86}Rb^+$ efflux assays as described previously.[23,71] In brief, cells were plated into 24-well plates coated with poly-D-lysine. The plated cells were grown at 37 °C for 18 to 24 h to reach 85−95% confluence. The cells were then incubated in growth medium (0.5 mL/well) containing $^{86}Rb^+$ (2 μCi/mL) for 4 h at 37 °C. The loading mixture was then aspirated, and the cells were washed four times with 1 mL of buffer (15 mM HEPES, 140 mM NaCl, 2 mM KCl, 1 mM $MgSO_4$, 1.8 mM $CaCl_2$, 11 mM glucose, pH 7.4). Then 1 mL of buffer with or without compounds to be tested was added to each well. After incubation for 2 min, the assay buffer was collected for measurements of $^{86}Rb^+$ released from the cells. Cells were then lysed by adding 1 mL of 100 mM NaOH to each well, and the lysate was collected for determination of the amount of $^{86}Rb^+$ that was in the cells at the end of the efflux assay. Radioactivity of assay samples and lysates was measured by liquid scintillation counting. Total loading (cpm) was calculated as the sum of the assay sample and the lysate of each well. The amount of $^{86}Rb^+$ efflux was expressed as a percentage of $^{86}Rb^+$ loaded. Stimulated $^{86}Rb^+$ efflux was defined as the difference between efflux in the presence and absence of nicotine. For obtaining EC_{50} and E_{max} values, stimulation curves were constructed in which eight different concentrations of a ligand were included in the assay. For obtaining an $IC_{50(10')}$ value, inhibition curves were constructed in which eight different concentrations of a compound were applied to cells for 10 min before 100 μM nicotine was applied to measure stimulated efflux. EC_{50}, E_{max}, and $IC_{50(10')}$ values were determined by nonlinear least-squares regression analyses (GraphPad, San Diego, CA).

Electrophysiological Studies. Whole-cell voltage clamp (holding potential −70 mV) recordings were made from YXα4β2H1 cells. For increasing functionality of cells, cells were treated with 1 mM carbachol for 48 h before studies. The recordings were made with patch electrodes (5−6 MΩ) containing a solution composed of (in mM; pH 7.2): K gluconate (145), EGTA (5), $MgCl_2$ (2.5), HEPES (10), ATP·Na (5), and GTP·Na (0.2). Cells were continuously perfused with recording solution having the following composition (mM): NaCl (130), KCl (5), $CaCl_2$ (2), $MgCl_2$ (2), glucose (10), and HEPES (10), pH 7.4, at a temperature of 24 °C. They were visually identified by infrared-differential interference contrast (IR-DIC) optics via a CCD camera (Dage S-75). A 60× water immersion objective (Nikon) was used for identifying and approaching cells. Only one cell per coverslip was recorded.

The patch pipet was coupled to an amplifier (Axopatch 700B; Axon Instruments Inc.) and its signal filtered (5kHz), digitized (Digidata 1440A; Axon Instruments Inc.), and stored on a PC computer running the pClamp 10 software (Axon Instruments Inc.) for later analysis. Series resistance was typically <10 MΩ and was continuously monitored with a 10 mV pulse.

Acetylcholine (32 μM) was delivered by rapid focal application (500 ms; pressure ∼15 psi), whereas compound **1** (200nM) was applied via bath application. The whole-cell current response to compound **1** was normalized in relation to two stable prior applications of the 32 μM ACh-induced responses (interstimulus interval 5 min).

Brain Tissue and Plasma Protein Binding Studies. Briefly, each test compound at a concentration of 5 μM is incubated in plasma or homogenized brain tissue in a RED equilibrium dialysis device and dialyzed against PBS using the published procedure.[75] After 4 h, each side is analyzed for test agent by LC/MS/MS. From this, the free drug in brain, free in plasma, and brain/plasma partitioning is calculated using this equation $f_{Umeans} = 1 - \{(PC - PF)/PC\}$ PC = test compound concentration in protein-containing compartment, PF = test compound concentration in protein-free compartment, $f_{UBrain} = 1/D\ \{(1/f_{Umeans}) - 1 + 1/D\}$.

General Procedures for Animal Behavioral Studies. Separate sets of young adult female Sprague−Dawley rats were used for the nicotine self-administration study (N = 15) and for the locomotor activity study (N = 12). The studies were conducted in accordance with the regulations outlined by the Duke University Animal Care and Use Committee. The rats housed in approved standard laboratory conditions in a Duke University vivarium facility near the testing room to minimize stress induced by transporting the rats. The rats were kept on a 12:12 reverse day/night cycle so that they were in their active phase during behavioral testing. The rats in the drug iv self-administration studies were singly housed to prevent them from damaging each other's catheters. The rats in the locomotor activity studies were housed in groups of 2−3. All rats were allowed access to water at all times; the rats in the nicotine-self-administration study were fed daily approximately 30 min after completing the sessions while those in the locomotor activity study had continuous access to food.

Compound 1 Administration. Compound **1** was injected sc 10 min before testing in a volume of 1 mL/kg of saline. The doses (0, 0.3, 1, and 3 mg/kg) we given in a counterbalanced order with at least two days between successive injections. For the nicotine self-administration study, the compound **1** the acute dose−effect study was tested twice while for the locomotor activity study the dose−effect function was tested once.

Nicotine Self-Administration. Before beginning nicotine self-administration, the rats were trained for three sessions on lever pressing for food reinforcement. Then they were fitted with iv catheters, and they received nicotine infusions (0.03 mg/kg/infusion) on an FR1 schedule for 10 sessions. The rats were trained to self-administer nicotine (0.03 mg/kg/infusion, IV) via operant lever response (FR1) with a visual secondary reinforcer. Two levers were available to be pressed, and only one caused the delivery of nicotine on an FR1 schedule. Pressing the lever on the active side resulted in the activation of the feedback tone for 0.5 s and the immediate delivery of one 50 μL infusion of nicotine in less than 1 s. Each infusion was immediately followed by a 1 min period in which the cue lights went out, the house light came on and responses were recorded but not reinforced.[28]

Locomotor Activity. Another set of rats (N = 12) was tested for acute compound **1** effects on locomotor activity in a figure-eight maze over the course of a 1 h session. The mazes had continuous enclosed alleys 10 cm × 10 cm in the shape of a figure eight.[76] The dimensions of the apparatus were 70 cm long and 42 cm wide, with a 21 cm × 16 cm central arena, a 20 cm high ceiling, and two blind alleys extending 20 cm from either side. Eight infrared photobeams, which crossed the alleys, indexed locomotor activity. One photobeam was located on each of the two blind alleys, and three were located on each of two loops of the figure eight. Numbers of photobeam breaks were recorded for 5 min blocks over the 1 h session. The repeated measures were compound **1** dose and the repeated administration of each dose. Significant interactions were followed up by tests of the simple main effects. Alpha of $p < 0.05$ (two-tailed) was used as the threshold for significance.

Physicochemical Properties and Ligand Efficiency. Molecular properties of compounds in series 1 were calculated according the available software tools. Ligand binding efficiency was calculated according to the Hopkins equation: LE = 1.372 × (−log K_i (moles))/N. Molecular weight and cLogP were calculated from Chembiodraw Ultra 11.0. Polar surface area (PSA) was calculated from www.chemicalize.org. Log BB was calculated from the following equation: Log BB = −0.0148PSA + 0.152CLogP + 0.139.

■ ASSOCIATED CONTENT

Ⓢ Supporting Information

Details of broad screening data, functional assay, and experimental details of intermediate compound synthesis.

This material is available free of charge via the Internet at http://pubs.acs.org.

■ AUTHOR INFORMATION

Corresponding Author

*Phone: +1-202-687-8603. Fax: +1-202-687-7659. Email: mb544@georgetown.edu.

Notes

The authors declare the following competing financial interest(s): A patent application has been filed by Georgetown University to claim commercial rights of inventions in this work. The following authors were listed on the patent application as inventors: V.M.Y., Y.X., E.D.L., A.H.R., M.P., K.J.K., and M.L.B.

■ ACKNOWLEDGMENTS

This work was supported by the National Institutes of Health grant DA02799 and by the Georgetown University Center for Drug Discovery. We thank the National Institute of Mental Health Psychoactive Drug Screening Program for performing binding assays at targets other than nAChRs.

■ ABBREVIATIONS USED

nAChR(s), nicotinic acetylcholine receptor(s); CNS, central nervous system; 5-HT, serotonin; GABA, γ-aminobutyric acid; AChBP, acetylcholine binding protein; ADME, absorption, metabolism, distribution, metabolism; SAR, structure−activity relationship

■ REFERENCES

(1) Gotti, C.; Riganti, L.; Vailati, S.; Clementi, F. Brain neuronal nicotinic receptors as new targets for drug discovery. *Curr. Pharm. Des.* **2006**, *12*, 407−428.

(2) Romanelli, M. N.; Gratteri, P.; Guandalini, L.; Martini, E.; Bonaccini, C.; Gualtieri, F. Central nicotinic receptors: structure, function, ligands, and therapeutic potential. *ChemMedChem.* **2007**, *2*, 746−767.

(3) Bunnelle, W. H.; Dart, M. J.; Schrimpf, M. R. Design of ligands for the nicotinic acetylcholine receptors: the quest for selectivity. *Curr. Top. Med. Chem.* **2004**, *4*, 299−334.

(4) Arneric, S. P.; Holladay, M.; Williams, M. Neuronal nicotinic receptors: a perspective on two decades of drug discovery research. *Biochem. Pharmacol.* **2007**, *74*, 1092−1101.

(5) Lindstrom, J.; Anand, R.; Peng, X.; Gerzanich, V.; Wang, F.; Li, Y. Neuronal nicotinic receptor subtypes. *Ann. N. Y. Acad. Sci.* **1995**, *757*, 100−116.

(6) Boyd, R. T. The molecular biology of neuronal nicotinic acetylcholine receptors. *Crit. Rev. Toxicol.* **1997**, *27*, 299−318.

(7) Gotti, C.; Clementi, F.; Fornari, A.; Gaimarri, A.; Guiducci, S.; Manfredi, I.; Moretti, M.; Pedrazzi, P.; Pucci, L.; Zoli, M. Structural and functional diversity of native brain neuronal nicotinic receptors. *Biochem. Pharmacol.* **2009**, *78*, 703−711.

(8) Kellar, K. J.; Xiao, Y. Neuronal nicotinic receptors: one hundred years of progress. In *Handbook of Contemporary Neuropharmacology*; John Wiley & Sons, Inc: Hoboken, NJ, 2007; pp 107−145.

(9) Mao, D.; Yasuda, R. P.; Fan, H.; Wolfe, B. B.; Kellar, K. J. Heterogeneity of nicotinic cholinergic receptors in rat superior cervical and nodose Ganglia. *Mol. Pharmacol.* **2006**, *70*, 1693−1699.

(10) Pidoplichko, V. I.; DeBiasi, M.; Williams, J. T.; Dani, J. A. Nicotine activates and desensitizes midbrain dopamine neurons. *Nature* **1997**, *390*, 401−404.

(11) Nestler, E. J. Is there a common molecular pathway for addiction? *Nature Neurosci.* **2005**, *8*, 1445−1449.

(12) Picciotto, M. R.; Zoli, M.; Rimondini, R.; Lena, C.; Marubio, L. M.; Pich, E. M.; Fuxe, K.; Changeux, J. P. Acetylcholine receptors containing the beta2 subunit are involved in the reinforcing properties of nicotine. *Nature* **1998**, *391*, 173−177.

(13) Marubio, L. M.; Gardier, A. M.; Durier, S.; David, D.; Klink, R.; Arroyo-Jimenez, M. M.; McIntosh, J. M.; Rossi, F.; Champtiaux, N.; Zoli, M.; Changeux, J. P. Effects of nicotine in the dopaminergic system of mice lacking the alpha4 subunit of neuronal nicotinic acetylcholine receptors. *Eur. J. Neurosci.* **2003**, *17*, 1329−1337.

(14) Maskos, U.; Molles, B. E.; Pons, S.; Besson, M.; Guiard, B. P.; Guilloux, J. P.; Evrard, A.; Cazala, P.; Cormier, A.; Mameli-Engvall, M.; Dufour, N.; Cloez-Tayarani, I.; Bemelmans, A. P.; Mallet, J.; Gardier, A. M.; David, V.; Faure, P.; Granon, S.; Changeux, J. P. Nicotine reinforcement and cognition restored by targeted expression of nicotinic receptors. *Nature* **2005**, *436*, 103−107.

(15) Dani, J. A.; Heinemann, S. Molecular and cellular aspects of nicotine abuse. *Neuron* **1996**, *16*, 905−908.

(16) Rollema, H.; Coe, J. W.; Chambers, L. K.; Hurst, R. S.; Stahl, S. M.; Williams, K. E. Rationale, pharmacology and clinical efficacy of partial agonists of alpha4beta2 nACh receptors for smoking cessation. *Trends Pharmacol. Sci.* **2007**, *28*, 316−325.

(17) Gonzales, D.; Rennard, S. I.; Nides, M.; Oncken, C.; Azoulay, S.; Billing, C. B.; Watsky, E. J.; Gong, J.; Williams, K. E.; Reeves, K. R. Varenicline, an alpha4beta2 nicotinic acetylcholine receptor partial agonist, vs sustained-release bupropion and placebo for smoking cessation: a randomized controlled trial. *JAMA, J. Am. Med. Assoc.* **2006**, *296*, 47−55.

(18) Jorenby, D. E.; Hays, J. T.; Rigotti, N. A.; Azoulay, S.; Watsky, E. J.; Williams, K. E.; Billing, C. B.; Gong, J.; Reeves, K. R. Efficacy of varenicline, an alpha4beta2 nicotinic acetylcholine receptor partial agonist, vs placebo or sustained-release bupropion for smoking cessation: a randomized controlled trial. *JAMA, J. Am. Med. Assoc.* **2006**, *296*, 56−63.

(19) Tonstad, S.; Tonnesen, P.; Hajek, P.; Williams, K. E.; Billing, C. B.; Reeves, K. R. Effect of maintenance therapy with varenicline on smoking cessation: a randomized controlled trial. *JAMA, J. Am. Med. Assoc.* **2006**, *296*, 64−71.

(20) Tsai, S. T.; Cho, H. J.; Cheng, H. S.; Kim, C. H.; Hsueh, K. C.; Billing, C. B., Jr.; Williams, K. E. A randomized, placebo-controlled trial of varenicline, a selective alpha4beta2 nicotinic acetylcholine receptor partial agonist, as a new therapy for smoking cessation in Asian smokers. *Clin. Ther.* **2007**, *29*, 1027−1039.

(21) Moore, T. J.; Furberg, C. D.; Glenmullen, J.; Maltsberger, J. T.; Singh, S. Suicidal behavior and depression in smoking cessation treatments. *PLoS One* **2011**, *6*, e27016.

(22) Rollema, H.; Chambers, L. K.; Coe, J. W.; Glowa, J.; Hurst, R. S.; Lebel, L. A.; Lu, Y.; Mansbach, R. S.; Mather, R. J.; Rovetti, C. C.; Sands, S. B.; Schaeffer, E.; Schulz, D. W.; Tingley, F. D., III; Williams, K. E. Pharmacological profile of the alpha4beta2 nicotinic acetylcholine receptor partial agonist varenicline, an effective smoking cessation aid. *Neuropharmacology.* **2007**, *52*, 985−994.

(23) Mihalak, K. B.; Carroll, F. I.; Luetje, C. W. Varenicline is a partial agonist at alpha4beta2 and a full agonist at alpha7 neuronal nicotinic receptors. *Mol. Pharmacol.* **2006**, *70*, 801−805.

(24) Bordia, T.; Hrachova, M.; Chin, M.; McIntosh, J. M.; Quik, M. Varenicline is a potent partial agonist at alpha6beta2* nicotinic acetylcholine receptors in rat and monkey striatum. *J. Pharmacol. Exp. Ther.* **2012**, *342*, 327−334.

(25) Xiao, Y.; Fan, H.; Musachio, J. L.; Wei, Z. L.; Chellappan, S. K.; Kozikowski, A. P.; Kellar, K. J. Sazetidine-A, a novel ligand that desensitizes alpha4beta2 nicotinic acetylcholine receptors without activating them. *Mol. Pharmacol.* **2006**, *70*, 1454−1460.

(26) Xiao, Y.; Yasuda, R. P.; Sahibzada, N.; Wolfe, B. B.; Horton, L.; Paige, M.; Brown, M. L.; Kellar, K. J. Sazetidine-A selectively induces a long lasting desensitization of $\alpha4\beta2$ nicotinic acetylcholine receptors. In (), 2010 Neuroscience Meeting, Society for Neuroscience, San Diego, 2010, 38.10.

(27) Carbone, A. L.; Moroni, M.; Groot-Kormelink, P. J.; Bermudez, I. Pentameric concatenated (alpha4)(2)(beta2)(3) and (alpha4)(3)(beta2)(2) nicotinic acetylcholine receptors: subunit arrangement

determines functional expression. *Br. J. Pharmacol.* **2009**, *156*, 970−981.
(28) Levin, E. D.; Rezvani, A. H.; Xiao, Y.; Slade, S.; Cauley, M.; Wells, C.; Hampton, D.; Petro, A.; Rose, J. E.; Brown, M. L.; Paige, M. A.; McDowell, B. E.; Kellar, K. J. Sazetidine-A, a selective alpha4beta2 nicotinic receptor desensitizing agent and partial agonist, reduces nicotine self-administration in rats. *J. Pharmacol. Exp. Ther.* **2010**, *332*, 933−939.
(29) Rezvani, A. H.; Slade, S.; Wells, C.; Petro, A.; Lumeng, L.; Li, T. K.; Xiao, Y.; Brown, M. L.; Paige, M. A.; McDowell, B. E.; Rose, J. E.; Kellar, K. J.; Levin, E. D. Effects of sazetidine-A, a selective alpha4beta2 nicotinic acetylcholine receptor desensitizing agent on alcohol and nicotine self-administration in selectively bred alcohol-preferring (P) rats. *Psychopharmacology (Berlin, Ger.)* **2010**, *211*, 161−174.
(30) Rezvani, A. H.; Cauley, M.; Sexton, H.; Xiao, Y.; Brown, M. L.; Paige, M. A.; McDowell, B. E.; Kellar, K. J.; Levin, E. D. Sazetidine-A, a selective alpha4beta2 nicotinic acetylcholine receptor ligand: effects on dizocilpine and scopolamine-induced attentional impairments in female Sprague-Dawley rats. *Psychopharmacology (Berlin, Ger.)* **2011**, *215*, 621−630.
(31) Kozikowski, A. P.; Eaton, J. B.; Bajjuri, K. M.; Chellappan, S. K.; Chen, Y.; Karadi, S.; He, R.; Caldarone, B.; Manzano, M.; Yuen, P. W.; Lukas, R. J. Chemistry and pharmacology of nicotinic ligands based on 6-[5-(azetidin-2-ylmethoxy)pyridin-3-yl]hex-5-yn-1-ol (AMOP-H-OH) for possible use in depression. *ChemMedChem* **2009**, *4*, 1279−1291.
(32) Turner, J. R.; Castellano, L. M.; Blendy, J. A. Nicotinic partial agonists varenicline and sazetidine-A have differential effects on affective behavior. *J. Pharmacol. Exp. Ther.* **2010**, *334*, 665−672.
(33) Caldarone, B. J.; Wang, D.; Paterson, N. E.; Manzano, M.; Fedolak, A.; Cavino, K.; Kwan, M.; Hanania, T.; Chellappan, S. K.; Kozikowski, A. P.; Olivier, B.; Picciotto, M. R.; Ghavami, A. Dissociation between duration of action in the forced swim test in mice and nicotinic acetylcholine receptor occupancy with sazetidine, varenicline, and 5-I-A85380. *Psychopharmacology (Berlin, Ger.)* **2011**, *217*, 199−210.
(34) Hussmann, G. P.; Kellar, K. J. A new radioligand binding assay to measure the concentration of drugs in rodent brain ex vivo. *J. Pharmacol. Exp. Ther.* **2012**, *343*, 434−440.
(35) Severin, R.; Reimer, J.; Doye, S. One-pot procedure for the synthesis of unsymmetrical diarylalkynes. *J. Org. Chem.* **2010**, *75*, 3518−3521.
(36) Holladay, M. W.; Bai, H.; Li, Y.; Lin, N. H.; Daanen, J. F.; Ryther, K. B.; Wasicak, J. T.; Kincaid, J. F.; He, Y.; Hettinger, A. M.; Huang, P.; Anderson, D. J.; Bannon, A. W.; Buckley, M. J.; Campbell, J. E.; Donnelly-Roberts, D. L.; Gunther, K. L.; Kim, D. J.; Kuntzweiler, T. A.; Sullivan, J. P.; Decker, M. W.; Arneric, S. P. Structure−activity studies related to ABT-594, a potent nonopioid analgesic agent: effect of pyridine and azetidine ring substitutions on nicotinic acetylcholine receptor binding affinity and analgesic activity in mice. *Bioorg. Med. Chem. Lett.* **1998**, *8*, 2797−2802.
(37) Huang, X.; Zheng, F.; Crooks, P. A.; Dwoskin, L. P.; Zhan, C. G. Modeling multiple species of nicotine and deschloroepibatidine interacting with alpha4beta2 nicotinic acetylcholine receptor: from microscopic binding to phenomenological binding affinity. *J. Am. Chem. Soc.* **2005**, *127*, 14401−14414.
(38) Karlin, A. Emerging structure of the nicotinic acetylcholine receptors. *Nature Rev. Neurosci.* **2002**, *3*, 102−114.
(39) Karlin, A. A touching picture of nicotinic binding. *Neuron* **2004**, *41*, 841−842.
(40) Lester, H. A.; Dibas, M. I.; Dahan, D. S.; Leite, J. F.; Dougherty, D. A. Cys-loop receptors: new twists and turns. *Trends Neurosci.* **2004**, *27*, 329−336.
(41) Unwin, N. Refined structure of the nicotinic acetylcholine receptor at 4A resolution. *J. Mol. Biol.* **2005**, *346*, 967−989.
(42) Brejc, K.; van Dijk, W. J.; Klaassen, R. V.; Schuurmans, M.; van Der, O. J.; Smit, A. B.; Sixma, T. K. Crystal structure of an AChBP binding protein reveals the ligand-binding domain of nicotinic receptors. *Nature* **2001**, *411*, 269−276.
(43) Celie, P. H.; Rossum-Fikkert, S. E.; van Dijk, W. J.; Brejc, K.; Smit, A. B.; Sixma, T. K. Nicotine and carbamylcholine binding to nicotinic acetylcholine receptors as studied in AChBP crystal structures. *Neuron* **2004**, *41*, 907−914.
(44) Chico, L. K.; Van Eldik, L. J.; Watterson, D. M. Targeting protein kinases in central nervous system disorders. *Nature Rev. Drug Discovery* **2009**, *8*, 892−909.
(45) Pajouhesh, H.; Lenz, G. R. Medicinal chemical properties of successful central nervous system drugs. *NeuroRx* **2005**, *2*, 541−553.
(46) Reichel, A. Addressing central nervous system (CNS) penetration in drug discovery: basics and implications of the evolving new concept. *Chem. Biodiversity* **2009**, *6*, 2030−2049.
(47) Ghose, A. K.; Herbertz, T.; Hudkins, R. L.; Dorsey, B. D.; Mallamo, J. P. Knowledge-Based, Central Nervous System (CNS) Lead Selection and Lead Optimization for CNS Drug Discovery. *ACS Chem. Neurosci.* **2012**, *3*, 50−68.
(48) Goodwin, J. T.; Clark, D. E. In silico predictions of blood-brain barrier penetration: considerations to "keep in mind". *J. Pharmacol. Exp. Ther.* **2005**, *315*, 477−483.
(49) Clark, D. E. Rapid calculation of polar molecular surface area and its application to the prediction of transport phenomena. 2. Prediction of blood−brain barrier penetration. *J. Pharm. Sci.* **1999**, *88*, 815−821.
(50) Abad-Zapatero, C.; Perisic, O.; Wass, J.; Bento, A. P.; Overington, J.; Al-Lazikani, B.; Johnson, M. E. Ligand efficiency indices for an effective mapping of chemico-biological space: the concept of an atlas-like representation. *Drug Discovery Today* **2010**, *15*, 804−811.
(51) Hopkins, A. L.; Groom, C. R.; Alex, A. Ligand efficiency: a useful metric for lead selection. *Drug Discovery Today* **2004**, *9*, 430−431.
(52) Hajek, P.; McRobbie, H.; Myers, K. Efficacy of cytisine in helping smokers quit: systematic review and meta-analysis. *Thorax.* **2013**, DOI: 10.1136/thoraxjnl-2012-203035.
(53) Freedman, R. Exacerbation of schizophrenia by varenicline. *Am. J. Psychiatry* **2007**, *164*, 1269.
(54) Kohen, I.; Kremen, N. Varenicline-induced manic episode in a patient with bipolar disorder. *Am. J. Psychiatry* **2007**, *164*, 1269−1270.
(55) Singh, S.; Loke, Y. K.; Spangler, J. G.; Furberg, C. D. Risk of serious adverse cardiovascular events associated with varenicline: a systematic review and meta-analysis. *Can. Med. Assoc. J.* **2011**, *183*, 1359−1366.
(56) Coe, J. W.; Brooks, P. R.; Vetelino, M. G.; Wirtz, M. C.; Arnold, E. P.; Huang, J.; Sands, S. B.; Davis, T. I.; Lebel, L. A.; Fox, C. B.; Shrikhande, A.; Heym, J. H.; Schaeffer, E.; Rollema, H.; Lu, Y.; Mansbach, R. S.; Chambers, L. K.; Rovetti, C. C.; Schulz, D. W.; Tingley, F. D., III; O'Neill, B. T. Varenicline: an alpha4beta2 nicotinic receptor partial agonist for smoking cessation. *J. Med. Chem.* **2005**, *48*, 3474−3477.
(57) Lummis, S. C.; Thompson, A. J.; Bencherif, M.; Lester, H. A. Varenicline is a potent agonist of the human 5-hydroxytryptamine3 receptor. *J. Pharmacol. Exp. Ther.* **2011**, *339*, 125−131.
(58) Johnson, J. E.; Slade, S.; Wells, C.; Petro, A.; Sexton, H.; Rezvani, A. H.; Brown, M. L.; Paige, M. A.; McDowell, B. E.; Xiao, Y.; Kellar, K. J.; Levin, E. D. Assessing the effects of chronic sazetidine-A delivery on nicotine self-administration in both male and female rats. *Psychopharmacology (Berlin, Ger.)* **2012**, *222*, 269−276.
(59) Cucchiaro, G.; Xiao, Y.; Gonzalez-Sulser, A.; Kellar, K. J. Analgesic effects of sazetidine-A, a new nicotinic cholinergic drug. *Anesthesiology* **2008**, *109*, 512−519.
(60) AlSharari, S. D.; Carroll, F. I.; McIntosh, J. M.; Damaj, M. I. The antinociceptive effects of nicotinic partial agonists varenicline and sazetidine-A in murine acute and tonic pain models. *J. Pharmacol. Exp. Ther.* **2012**, *342*, 742−749.
(61) Liu, J.; Eaton, J. B.; Caldarone, B.; Lukas, R. J.; Kozikowski, A. P. Chemistry and pharmacological characterization of novel nitrogen analogues of AMOP-H-OH (sazetidine-A, 6-[5-(azetidin-2-

ylmethoxy)pyridin-3-yl]hex-5-yn-1-ol) as alpha4beta2-nicotinic acetylcholine receptor-selective partial agonists. *J. Med. Chem.* **2010**, *53*, 6973−6985.

(62) Fiser, A.; Do, R. K.; Sali, A. Modeling of loops in protein structures. *Protein Sci.* **2000**, *9*, 1753−1773.

(63) Altschul, S. F.; Gish, W.; Miller, W.; Myers, E. W.; Lipman, D. J. Basic local alignment search tool. *J. Mol. Biol.* **1990**, *215*, 403−410.

(64) Chenna, R.; Sugawara, H.; Koike, T.; Lopez, R.; Gibson, T. J.; Higgins, D. G.; Thompson, J. D. Multiple sequence alignment with the Clustal series of programs. *Nucleic Acids Res.* **2003**, *31*, 3497−3500.

(65) Case, D. A.; Darden, T. A.; Cheatham, T. E.; Simmerling, C. L.; Wang, J.; Duke, R. E.; Luo, R.; Merz, K. M.; Pearlman, D. A.; Crowley, M.; Walker, R. C.; Zhang, W.; Wang, B.; Hayik, S.; Roitberg, A.; Seabra, G.; Wong, K. F.; Paesani, F.; Wu, X.; Brozell, S.; Tsui, V.; Gohlke, H.; Yang, L.; Tan, C.; Mongan, J.; Hornak, V.; Cui, G.; Beroza, P.; Mathews, D. H.; Schafmeister, C.; Ross, W. S.; Kollman, P. A. *AMBER 9*; University of California: San Francisco, 2006.

(66) Laskowski, R. A.; MacArthur, M. W.; Moss, D. S.; Thornton, J. M. *PROCHECK*: a program to check the stereochemical quality of protein structure. *J. Appl. Crystallogr.* **1993**, *26*, 283−291.

(67) Vriend, G. WHAT IF: a molecular modeling and drug design program. *J. Mol. Graphics* **1990**, *8*, 52−56.

(68) Frisch, M. J.; Trucks, G. W.; Cheeseman, J. R.; Scalmani, G.; Caricato, M.; Hratchian, H. P.; Li, X.; Barone, V.; Bloino, J.; Zheng, G.; Vreven, T.; Montgomery, Jr. J. A.; Petersson, G. A.; Scuseria, G. E.; Schlegel, H. B.; Nakatsuji, H.; zmaylov, A. F.; Martin, R. L.; Sonnenberg, J. L.; Peralta, J. E.; Heyd, J. J.; Brothers, E.; Ogliaro, F.; Bearpark, M.; Robb, M. A.; Mennucci, B.; Kudin, K. N.; Staroverov, V. N.; Kobayashi, R.; Normand, J.; Rendell, A.; Gomperts, R.; Zakrzewski, V. G.; Hada, M.; Ehara, M.; Toyota, K.; Fukuda, R.; Hasegawa, J.; Ishida, M.; Nakajima, T.; Honda, Y.; Kitao O.; Nakai, H. *Gaussian 09*; Gaussian, Inc.: Wallingford, CT, 2009.

(69) Hanson, R. N.; Lee, C. Y.; Friel, C. J.; Dilis, R.; Hughes, A.; DeSombre, E. R. Synthesis and evaluation of 17alpha-20*E*-21-(4-substituted phenyl)-19-norpregna-1,3,5(10),20-tetraene-3,17beta-diols as probes for the estrogen receptor alpha hormone binding domain. *J. Med. Chem.* **2003**, *46*, 2865−2876.

(70) Berendsen, H. J.C.; Postma, J. P. M.; vanGunsteren, W. F.; DiNola, A.; Haak, J. R. Molecular dynamics with coupling to an external bath. *J. Chem. Phys.* **1984**, *81*, 3684.

(71) Darden, T.; York, D.; Pedersen, L. Particle mesh Ewald: An $N\cdot\log(N)$ method for Ewald sums in large systems. *J. Chem. Phys.* **1993**, *98*, 10089.

(72) Xiao, Y.; Kellar, K. J. The comparative pharmacology and up-regulation of rat neuronal nicotinic receptor subtype binding sites stably expressed in transfected mammalian cells. *J. Pharmacol. Exp. Ther.* **2004**, *310*, 98−107.

(73) Xiao, Y.; Meyer, E. L.; Thompson, J. M.; Surin, A.; Wroblewski, J.; Kellar, K. J. Rat alpha3/beta4 subtype of neuronal nicotinic acetylcholine receptor stably expressed in a transfected cell line: pharmacology of ligand binding and function. *Mol. Pharmacol.* **1998**, *54*, 322−333.

(74) Xiao, Y.; Abdrakhmanova, G. R.; Baydyuk, M.; Hernandez, S.; Kellar, K. J. Rat neuronal nicotinic acetylcholine receptors containing alpha7 subunit: pharmacological properties of ligand binding and function. *Acta Pharmacol. Sin.* **2009**, *30*, 842−850.

(75) Maurer, T. S.; Debartolo, D. B.; Tess, D. A.; Scott, D. O. Relationship between exposure and nonspecific binding of thirty-three central nervous system drugs in mice. *Drug Metab. Dispos.* **2005**, *33*, 175−181.

(76) Crofton, K. M.; Howard, J. L.; Moser, V. C.; Gill, M. W.; Reiter, L. W.; Tilson, H. A.; MacPhail, R. C. Interlaboratory comparison of motor activity experiments: implications for neurotoxicological assessments. *Neurotoxicol. Teratol.* **1991**, *13*, 599−609.